



PONTIFICIA UNIVERSIDAD CATÓLICA DE CHILE  
FACULTY OF MEDICINE

**THE ROLE OF VEGF-R3 PATHWAY SWITCH INDUCED  
BY M2-LIKE TUMOUR ASSOCIATED MACROPHAGES  
ON THE DEVELOPMENT OF A  
PRO-METASTATIC PHENOTYPE IN  
PAPILLARY THYROID CARCINOMA**

BY

**SERGIO S. VARGAS-SALAS, MD**

Thesis submitted to the Faculty of Medicine in partial fulfilment of the requirements for the academic degree of Doctor of Philosophy in Medical Sciences

Director:

HERNÁN GONZÁLEZ, MD PhD.

Co-Director:

JUAN CARLOS ROA, MD MSc.

JONATHAN SLEEMAN, MA PhD.

Santiago de Chile, July 2020

© MMXX, Sergio S. Vargas-Salas



PONTIFICIA UNIVERSIDAD CATÓLICA DE CHILE  
FACULTY OF MEDICINE

---

Santiago de Chile, July 2020

© MMXX, Sergio S. Vargas-Salas

None of the materials provided on this thesis may be used, reproduced or transmitted, in whole or in part, in any form or by any means, electronic or mechanical, including photocopying or the use of any information storage and retrieval system, without permission in writing from the author.



PONTIFICIA UNIVERSIDAD CATÓLICA DE CHILE  
Programa de Doctorado en Ciencias Médicas  
Dirección de Investigación y Doctorado  
Escuela de Medicina

La Comisión Examinadora, constituida por los Profesores abajo firmantes, aprueba la Defensa Pública de la Tesis Doctoral titulada:

**“THE ROLE OF VEGF-R3 PATHWAY SWITCH INDUCED BY M2-LIKE TUMOUR ASSOCIATED MACROPHAGES ON THE DEVELOPMENT OF A PRO-METASTATIC PHENOTYPE IN PAPILLARY THYROID CARCINOMA”**

**Aprobación Defensa Pública:**

**SR. SERGIO S. VARGAS SALAS**

Calificándose el trabajo realizado, el manuscrito sometido y la defensa oral, con nota

( 7.0 ) siete coma cero.

Dr. Mauricio Cuello  
Director de Investigación y Doctorado  
Escuela de Medicina, PUC

Dra. Carolina Bizama  
Sub-Jefe  
Programa Doctorado en Ciencias Médicas  
Escuela de Medicina, PUC

Dr. Juan Carlos Roa  
Co-Director de Tesis  
Escuela de Medicina, PUC

Dr. Alexis Kalergis  
Profesor Evaluador Externo  
Facultad de Ciencias Biológicas, PUC

Dr. Bruno Nervi  
Profesor Evaluador Interno  
Escuela de Medicina, PUC

Dr. Felipe Heusser  
Decano  
Facultad de Medicina, PUC

Dr. Jorge Carvajal  
Jefe  
Programa Doctorado en Ciencias Médicas  
Escuela de Medicina, PUC

Dr. Hernán González  
Director de Tesis  
Escuela de Medicina

Dra. Viviana Montecinos  
Profesor Evaluador Interno  
Escuela de Medicina, PUC

Santiago, 15 de octubre de 2020

*Scientia nihil aliud est quam veritatis imago*

*(Science is but an image of the truth)*

**- Sir Francis Bacon -**

*Truth will sooner come out of error than*

*from confusion*

**- Sir Francis Bacon -**

## ACKNOWLEDGEMENTS

To all of you...

To my mentor, Prof. Hernán González. For this long road that we have passed together, and for the rest that we must walk to the future. For all those midnight calls, sharing awakening thoughts, daydreaming about crazy ideas. For those wine glasses that we tasted while you guided me with experience and wisdom. For your expertise and your counselling, looking for the excellence in every step of my academic training. For your unconditional friendship.

To my co-directors, Prof. Juan Carlos Roa and Prof. Jonathan Sleeman. For their engagement and academic support in every moment, being always disposed to contribute, with kindness and patience, to the excellence of this work.

To my friends, Prof. Bruno Nervi and Patricia Macanas. For giving me the opportunity to be part of your lab. For placing your trust in me. For all the times you believed in my capacities. For considering me as a participant member of your present and your future in clinical research.

To my PhD friends. For all those moments we have shared. For those evenings discussing about things that, by our own, no one known exactly their meaning, but together we did it. For your laughs, your intelligence and your friendship.

To all my thesis committee. For your deep commitment with this work. For being always there when I needed. For having always an alternative when problems came out. For your time and patience. For the unselfishness to share all your expertise and knowledge.

To my patients. For helping me to know different realities. For understanding that science is the pathway to solve their problems, and for giving me the opportunity to take your questions from the hospital to our lab.

To my parents and my sister. For training me in the pathway of the integrity, the effort, and the constancy. For teaching me that no goal is unreachable. For being my light to understand the mysteries of God. For helping me, day by day, to be a better person. For existing.

To all of you, simply thanks.

## CONTENTS

ACKNOWLEDGEMENTS .....	v
LIST OF FIGURES .....	ix
LIST OF SUPPLEMENTARY CONTENTS .....	xi
ABSTRACT .....	xii
1. INTRODUCTION .....	1
1.1 Lymph Node Metastasis and its relevance in Cancer .....	1
1.2 Papillary Thyroid Cancer as a model of Lymph Node Metastasis .....	3
1.3 The hypothesis of VEGF-R3 signalling switch .....	5
1.4 Tumour Associated Macrophages: their role on Lymph Node Metastasis and the VEGF-R3 signalling switch .....	7
1.5 A novel potential mechanism participating on Lymph Node Metastasis development in Papillary Thyroid Cancer .....	9
2. HYPOTHESIS .....	11
3. OBJECTIVES .....	12
4. METHODS .....	15
4.1 Patients and Specimens Collection .....	15
4.2 Cell Cultures .....	15
4.3 Immunophenotype characterisation .....	17
4.4 Transcriptomic and Proteomic assays .....	19
4.5 Migration and Invasion assays .....	22
4.6 Statistical Analysis .....	24
5. RESULTS .....	25
5.1 Metastatic PTC tumours show higher infiltration of M2-TAMs and no differences in M1-TAMs compared with non-metastatic tumours .....	25

5.2 M2-like macrophages isolated from PTC tumours have a differential transcriptomic profile in key cytokines compared with M1-like macrophages .....	25
5.3 Macrophages polarised in vitro display a differential transcriptomic profile in key cytokines comparable to the observed in ex vivo TAMs ...	26
5.4 M2-THP promote the expression of VEGF-R3 in TPC-1 but not in B-CPAP .....	28
5.5 In TPC-1, VEGF-R3 expressed after M2-THP stimulus is biologically active .....	29
5.6 M2-THP do not promote the secretion of VEGF-C in TPC-1 nor B-CPAP	30
5.7 M2-THP secrete significantly more VEGF-C compared with M1-THP and PTC cell lines .....	31
5.8 VEGF-C induces morphological changes in TPC-1 pre-incubated with CM-M2 but not in B-CPAP, consistent with a pro-metastatic phenotype .	31
5.9 VEGF-C promotes the expression of EMT genomic regulators in TPC-1 pre-incubated with CM-M2 but not in B-CPAP .....	32
5.10 VEGF-C promotes the migration capability in TPC-1 pre-incubated with CM-M2 but not in B-CPAP .....	35
6. DISCUSSION AND CONCLUSIONS .....	37
7. FIGURES .....	45
ABBREVIATIONS .....	75
BIBLIOGRAPHY .....	77
SUPPLEMENTARY CONTENTS .....	84

## LIST OF FIGURES

Figure 1: Schematisation of the LNM development process . . . . .	45
Figure 2: VEGF-R3 expression in samples of whole-tissue tumour from patients with NM-PTC and M-PTC . . . . .	46
Figure 3: VEGF-C transcript expression in samples of whole-tissue tumour from patients with NM-PTC and M-PTC . . . . .	47
Figure 4: VEGF-R3 expression in PTC cell lines . . . . .	48
Figure 5: VEGF-C transcript expression in PTC cell lines . . . . .	49
Figure 6: VEGF-R3 expression in PTC cell lines after TNF- $\alpha$ stimulus . . . . .	50
Figure 7: VEGF-C transcript expression in PTC cell lines after TNF- $\alpha$ stimulus . . . . .	51
Figure 8: Infiltration of M1-like and M2-like TAMs in primary tumours from NM-PTC and M-PTC . . . . .	52
Figure 9: Transcriptomic profile of key cytokines in TAMs isolated from NM-PTC and M-PTC primary tumours . . . . .	53
Figure 10: Phenotype changes of in vitro polarised macrophages . . . . .	55
Figure 11: Transcriptomic profile of key cytokines in TAMs polarised in vitro from THP-1 cells . . . . .	56
Figure 12: Transcriptomic profile of key cytokines in TAMs isolated from PTC primary tumours and TAMs polarised in vitro from THP-1 cells . . . . .	57
Figure 13: Effect of conditioned media from in vitro TAMs on VEGF-R3 expression in PTC cell lines . . . . .	59
Figure 14: Activation of VEGF-R3 expressed after incubation with conditioned media from in vitro TAMs . . . . .	60

Figure 15: Effect of conditioned media from in vitro TAMs on VEGF-C secretion in PTC cell lines .....	62
Figure 16: VEGF-C secretion by in vitro polarised TAMs .....	63
Figure 17: Phenotype changes in PTC cell lines after pre-incubation with conditioned medium from M2-THP and treatment with VEGF-C .....	64
Figure 18: Snail transcript expression induced by VEGF-C in PTC cell lines pre-incubated with conditioned media from in vitro TAMs .....	65
Figure 19: Slug transcript expression induced by VEGF-C in PTC cell lines pre-incubated with conditioned media from in vitro TAMs .....	67
Figure 20: Twist transcript expression induced by VEGF-C in PTC cell lines pre-incubated with conditioned media from in vitro TAMs .....	69
Figure 21: Effect of VEGF-C on migration capability in PTC cell lines incubated with conditioned medium from M1-THP .....	71
Figure 22: Effect of VEGF-C on migration capability in PTC cell lines incubated with conditioned medium from M2-THP .....	73

## LIST OF SUPPLEMENTARY CONTENTS

Number 1: VEGF-C transcriptomic profile in different organs for Homo sapiens	84
Number 2: Antibodies used for Cell Sorting .....	85
Number 3: Antibodies used for IHQ .....	86
Number 4: Primers used for Q-PCR .....	87
Number 5: Antibodies used for WB .....	88

## ABSTRACT

Cancer is the second leading cause of death globally. The major determinant of mortality in cancer patients is the presence of distant organ metastasis, and one of the most important clinical risk factors is the compromise of locoregional lymph nodes by cancer cells (lymph nodes metastasis or LNM). The pathogenesis of LNM includes many processes, and one of the main focuses of translational research in oncology has been the understanding of the biological mechanisms underlying those processes to develop novel diagnostic, prognostic and therapeutic clinical tools.

Among solid tumours, Papillary Thyroid Cancer (PTC) is an excellent model to study early events in LNM development, mainly due to three arguments: a significant number of samples can be potentially studied in a wide spectrum of the disease, from non-metastatic to widely invasive tumours; PTC is a well-differentiated tumour, so being possible to study early events in the cell transformation from a non-metastatic to a pro-metastatic phenotype; and PTC spreading occurs by lymphatic system in 95% of metastatic cases.

Previous background suggests that VEGF-R3/VEGF-C system could be an important signalling pathway by which epithelial tumours could develop a pro-metastatic architecture, not only by inducing the development of lymphatic vessels, but also by promoting the transformation of tumour epithelial cells to a pro-metastatic phenotype. Furthermore, M2-like tumour associated macrophages (M2-TAMs) seem to be key players in the pro-metastatic transformation as well. However, no previous studies have provided evidence suggesting that both, M2-TAMs and the VEGF-R3 pro-metastatic switch, could be associated. From prior results of our group, we postulate that, in PTC, M2-TAMs induce a VEGF-R3 pro-metastatic switch at the epithelial tumour cell, promoting the transformation toward a pro-metastatic phenotype. This work takes over two emerging questions aimed to confirm this hypothesis: which TAM subtype (M1-like or M2-like cells) induce a VEGF-R3 pro-metastatic switch in PTC?, and does the VEGF-

R3 pro-metastatic switch activate biological mechanisms that lead to a pro-metastatic phenotype in epithelial tumour cells?

Our results showed that conditioned medium from M2-TAM induces the overexpression of VEGF-R3 in TPC-1 (a non-metastatic PTC cell model) but not in B-CPAP (a metastatic PTC cell model), which suggest that the switch is a pre-metastatic event. Furthermore, the receptor is functionally active when cells are treated with VEGF-C (the specific ligand of VEGF-R3), inducing pro-metastatic morphological changes, the overexpression of genomic regulator of epithelial-to-mesenchymal transition, and increasing the cell migration capability. Taken together, these results support our working hypothesis; however, further studies are required to better understand the real meaning of this signalling pathway in the LNM development, as well as to determine the mechanisms by which M2-TAMs could induce the switch.

We expect that this work can help, in the future, to a better understanding of the mechanisms underlying the LNM development process in PTC, with potential applications in other solid tumours. Ultimately, this could be useful to generate important advances in diagnostic, prognostic and therapeutic tools, with potential impact in thousands of patients with cancer.

# 1. INTRODUCTION

## 1.1 Lymph Node Metastasis and its relevance in Cancer

Cancer is the second leading cause of death globally, being responsible for an estimated of 9.6 million deaths in 2018 (World Health Organization 2018). The major determinant of mortality in cancer patients is the presence of distant organ metastasis, which are mostly resistant to conventional therapies (Brody 2016). Across almost every tumour of epithelial origin, one of the most important clinical risk factors to develop distant organ metastasis is the compromise of locoregional lymph nodes by cancer cells (lymph nodes metastasis or LNM) (Gress 2017). In fact, therapeutic strategies are significantly more aggressive for patients with LNM and no distant organ metastasis, in order to reduce the risk to develop a systemic metastatic disease.

The pathogenesis of LNM includes many processes, and one of the main focuses of translational research in oncology has been the understanding of the biological mechanisms underlying those processes to develop novel diagnostic, prognostic and therapeutic clinical tools.

In brief, the three major components involved on the LNM development are described as follow (Joyce 2009, Raymond 2013, Pereira 2015) (figure 1):

- **Tumour niche changes:** the tumour niche, shaped by cancer cells coexisting with stromal cells, needs to be reorganised at cellular and molecular level, in order to foster three phenomena (in figure 1, light-yellow boxes);
  - Pro-Invasive phenotype transformation: cancer cells need to acquire an invasive and metastagenic phenotype, including detachment capability from the extra-cellular matrix (ECM) (Buchheit 2014), anoikis resistance (Simpson 2008) and epithelial-to-mesenchymal transition (EMT) (Thiery 2006, Polyak 2009).

- Lymphangiogenesis: the development of lymphatic vessels draining directly into the lymph nodes provides the anatomical route for cancer cells migration from the primary tumour site (Cao 2005, McColl 2005).
- Cancer-Endothelial cell interaction: the functional interaction between cancer cells and lymphatic endothelial cells is critical for intravasation (from the primary tumour to lymph) and extravasation (from lymph to the site of metastasis) (Saharinen 2004, Sleeman 2009).
- **Metastatic niche changes:** the metastatic niche, referred to the lymph node potentially invaded by cancer cells, display two pro-metastatic characteristics (in figure 1, light-green boxes);
  - Metastatic tropism: accumulated evidence suggests that cancer cells migration to lymph nodes is an active rather than passive process, driven by both, molecular and cellular factors (Zlotnik 2004), and not only by the anatomical lymphatic flow-draining of the tissue. That is, specific molecular and cellular factors could explain the metastatic preference by lymphatic instead of haematogenous pathway (Zlotnik 2006).
  - Pre-metastatic maturation: all the components of lymph node histological structure, including stromal cells and ECM, need to acquire a specific configuration in order to nest the metastatic cancer cells, as well as to allow their proper attachment, growth and proliferation (Fidler 2003, Fokas 2007).
- **Colonisation and Proliferation:** finally, once metastatic cancer cells arrive to the lymph node, they need to surpass the immune response, recognize the niche as proper for growing, and finally activate the mechanisms to consolidate the tumour proliferation and survival (Nguyen 2009, Massagué 2016), culminating the LNM development process (in figure 1, light-blue box).

Of these three components, the tumour niche changes could be considered as an early, necessary event in the LNM development aimed to be studied for diagnostic, prognostic

and therapeutic purposes. When analysing those phenomena fostered by the tumour niche changes, it seems clear that intra-tumour lymphangiogenesis is strongly associated with LNM (Zhang 2017). However, there are no significant differences in the density of lymphatic vessels infiltration between tumours with high and low LNM incidence rate (Wong 2006). Furthermore, no differences on the interaction between cells from different tumours and lymphatic endothelial cells have been described (Saharinen 2004). This suggests that, if some biological factor is involved on the preferred lymphatic spreading of some tumours, then it probably participates in the pro-metastatic phenotype transformation as well, besides the lymphangiogenesis and cancer-endothelial cell interaction. In other words, a biological mechanism that can be important as an early event in LNM development should participate in the pro-metastatic phenotype transformation, lymphangiogenesis and cancer-endothelial cell interaction<sup>1</sup>.

In the next sections, it is proposed a clinical model to study the LNM pathogenesis, as well as the scientific background supporting an alternative biological mechanism that could participate in the LNM development process.

## **1.2 Papillary Thyroid Cancer as a model of Lymph Node Metastasis**

Among solid tumours, Papillary Thyroid Cancer (PTC) has unique characteristics, emerging as an excellent clinical model to study the biological basis of LNM.

PTC is the most frequent endocrine malignancy (Pellegriti 2013), being the eighth cause of cancer in the US, and the fourth cause of cancer among women (Siegel 2016). The incidence of PTC has shown an exponential increase in the last three decades (Morris 2016), and it is expected that almost 30 cases per 100,000 will be diagnosed by 2030, from 15 cases per 100,000 diagnosed in 2014 (Rahib 2014). The rising of PTC diagnosis,

---

<sup>1</sup> Let this statement be considered as the most important argument for studying the VEGF-R3 signalling pathway.

mainly attributed to widespread detection of non-clinical tumours by ultrasound (Davies 2014), situates this disease as a public health problem. In this context, a significant number of samples can be potentially studied in a wide spectrum of the disease, from non-metastatic to widely invasive tumours<sup>2</sup>.

Physio-pathologically, PTC results from the malignant transformation of parenchymal cells of thyroid gland. When thyrocytes, a cuboidal epithelium representing over 85% of thyroid cells (Wartofsky 2000), turn to malignant, it could origin a tumour characterised by prominent microscopic papillae, specific nuclear features (optical clearing, grooves and eosinophilic inclusions), and calcium collections or psammoma bodies. Furthermore, since PTC is a well-differentiated tumour, it is possible to study early events in the cell transformation from a non-metastatic to a pro-metastatic phenotype<sup>3</sup>.

Finally, unlike other tumours, in which the rate of lymphatic metastasis (LNM) and haematogenous metastasis (distant organ metastasis) is variable, PTC spreading occurs by lymphatic system in 95% of metastatic cases<sup>4</sup>, invading cervical lymph nodes in most of them (Noguchi 1970). In fact, up to 30% of patients have clinical or image evidence of LNM, which will determine a more aggressive therapeutic strategy.

In summary, PTC emerges as an appropriate clinical model to study early events in the LNM development process. Furthermore, its high incidence is also an important factor, which makes possible to have a significant number of clinical samples for research.

---

<sup>2</sup> This is the first characteristic supporting the use of PTC as a clinical model for LNM development studying.

<sup>3</sup> This is the second characteristic supporting the use of PTC as a clinical model for LNM development studying.

<sup>4</sup> This is the third characteristic supporting the use of PTC as a clinical model for LNM development studying.

### 1.3 The hypothesis of VEGF-R3 pro-metastatic switch

Among different signalling pathways proposed as participants in the LNM development process, one of the main ones is the Vascular Endothelial Growth Factor Receptor 3 (VEGF-R3) signalling pathway. Briefly, the role of the VEGF gene family in the general metastatic process has been largely described since these genes predominantly encodes for pro-angiogenic and pro-lymphangiogenic receptors and ligands (Ferrara 2003). In particular, VEGF-R3 is well known as the master receptor regulating lymphangiogenesis (Zhang 2010), so being an excellent candidate to play a critical role on LNM development. Its ligands, VEGF-C and VEGF-D, have a highly selective affinity (135 pM and 0.79 pM, respectively) (Joukov 1997, McColl 2007), with VEGF-C being the most secreted ligand by far (Joukov 1997).

It has been proposed that tumours developing LNM could carry a switch in the expression of VEGF receptors and ligands, wherein VEGF-R3 and VEGF-C expression within the tumour microenvironment would be dominant. Usually, the primary VEGF profile is more associated with the expression of VEGF-R2 and VEGF-A, since this pathway is responsible for cell growth and angiogenesis (Abhinand 2016), both processes critical for tumour development. However, accumulated evidence has shown that, as tumour turns to more aggressive, the microenvironment displays a genomic/proteomic switch in the VEGF receptors and ligands profile, increasing the levels of VEGF-R3 and VEGF-C (Hanahan 1996, Relf 1997). Interestingly, this VEGF-R3 pro-metastatic switch<sup>5</sup> (Cao 2005) could be relevant beyond the lymphangiogenesis process. Previous results on colon and lung cancer cell lines (Khromova 2012) have shown that VEGF-R3 signalling at the epithelial tumour cell seem to uphold the selection of cancer stem cells, increase the mitotic rate, and promote the EMT, suggesting a novel role of VEGF-R3 on the LNM development.

---

<sup>5</sup> The VEGF-R3 pro-metastatic switch is defined, therefore, as the genomic/proteomic overexpression of VEGF-R3 and its ligand VEGF-C. Importantly, this switch is not defined by the functional activity of the VEGF-R3 signalling pathway, but rather the overexpression of its genomic/proteomic components.

Back to PTC as a research model for LNM, our group has been interested in elucidating whether the VEGF-R3 pro-metastatic switch participates in the epithelial tumour cell transformation from a non-metastatic to a pro-metastatic phenotype. As a first approach, based on *in silico* analyses from the HPA (Uhlén 2015) and GTEx (Keen 2015) databases, we found that thyroid gland is the organ expressing the highest basal levels of VEGF-C (measured by transcriptomic and proteomic assays) compared with others (supplementary content 1). This result suggests that in case the VEGF-R3 pro-metastatic switch were playing a role on the LNM development in PTC, the levels of VEGF-C needed to activate the signalling pathway would be already almost achieved, so making this organ more sensitive to LNM<sup>6</sup>. Considering this *in silico* result, we explored the existence of the VEGF-R3 pro-metastatic switch in PTC samples of whole-tissue primary tumour from patients with (M-PTC) and without (NM-PTC) LNM (30 per each group) by immunohistochemistry (IHQ) and real time polymerase chain reaction (Q-PCR). By IHQ, the number of epithelial cells positive for VEGF-R3 were 2.38-fold higher in M-PTC compared with NM-PTC (figure 2), while mRNA levels (from whole-tissue tumour lysate) of VEGF-C were augmented by 2.72-fold in M-PTC (figure 3). As a next step, we aimed to determine whether epithelial tumour cells could be responsible, at least partly, of that switch observed in whole-tissue tumour samples. *In vitro*, we studied two PTC cell lines (N = 6): TPC-1 (a RET/PTC1 positive PTC cell line isolated from a patient with non-metastatic, low-risk tumour) (Saiselet 2012) and B-CPAP (a BRAF-mutated PTC cell line isolated from a patient with several metastases and highly aggressive tumour) (Ribeiro 2008, Saiselet 2012)<sup>7</sup>. Consistent with our prior results, the expression of VEGF-R3 (measured by western-blotting -WB-) was higher in B-CPAP than TPC-1 by 2.06-fold (figure 4). Furthermore, the transcript levels of VEGF-C (measured by Q-PCR) were approximately 2.98-fold higher in B-CPAP than TPC-1 (figure 5). Together, these results suggest that the VEGF-R3 pro-metastatic switch is clinically observed in PTC; and that

---

<sup>6</sup> This would be consistent with the clinical observation that PTC is a tumour with a preferred lymphatic spreading.

<sup>7</sup> According to the origin of these cell lines, TPC-1 can be considered as a cell model of NM-PTC, and B-CPAP as a cell model of M-PTC.

the switch is observed at epithelial cell level in the PTC cell line model. Therefore, bioinformatics and experimental results support the hypothesis on the role of VEGF-R3 pro-metastatic switch (characterised by an overexpression of VEGF-R3 receptor and its ligand VEGF-C) in PTC LNM development.

#### **1.4 Tumour Associated Macrophages: their role on Lymph Node Metastasis and the VEGF-R3 signalling switch**

Accumulated evidence suggest that tumour microenvironment induce phenotype changes in the tumour cells, as well as an extracellular matrix remodelling, facilitating the metastatic process (Whiteside 2013). In this context, inflammatory cells seem to play a key role, since tumour cells produce multiple leukocyte-attractant molecules by intrinsic (i.e. due to genetic alterations) and extrinsic (i.e. due to chronic inflammatory stimulus) mechanisms (Conway 2016). One of the most important tumour-associated leukocytes are Tumour Associated Macrophages (TAM), which can display a wide activation spectrum, being M1 and M2 phenotypes the extremes of this spectrum<sup>8</sup> (Mantovani 2002, Mosser 2008).

When polarised to an M1-like cell in response to interferon gamma (IFN- $\gamma$ ) and granulocyte-macrophage colony-stimulating factor (GM-CSF), TAMs are characterised by a high production of pro-inflammatory cytokines (IL-12 and IL-23) (Ambarus 2012), and high expression of major histocompatibility complex class II (MHC-II) and co-activation proteins (CD80/86) (Mantovani 2010). M1-like macrophages (M1-TAM) promote tumorigenesis by producing reactive intermediates, tissue damage and releasing inflammatory cytokines, predisposing the surrounding epithelial cells to DNA damage and

---

<sup>8</sup> M1 and M2 phenotypes are theoretical approaches to TAMs polarisation. However, it is important to highlight that *in vivo* TAMs phenotype are a broad spectrum of cells with a variable similarity to one of those two poles, so being more appropriately named as M1-like or M2-like rather than pure M1 or M2 TAMs. In this manuscript, TAMs will be indistinctly named as M1/M1-like or M2/M2-like, but always under the prior consideration.

subsequent neoplastic transformation (pre-metastatic processes). Oppositely, macrophages are polarised to an M2-like phenotype (M2-TAM) in response to macrophage colony-stimulating factor (M-CSF) and anti-inflammatory cytokines (IL-4, IL-6 and IL-13) (Ambarus 2012), secreting a variety of anti-inflammatory cytokines, immunosuppressive mediators and matrix-degrading enzymes, which promotes angiogenesis and tissue remodelling and repair (pro-metastatic processes) (Mantovani 2004, Mantovani 2010)<sup>9</sup>.

In PTC, the importance of TAM (uncharacterised by their polarised phenotype)<sup>10</sup> on LNM development has been partially studied. When PTC primary tumour samples are histologically analysed, there is a positive and statistically significant correlation between the number of infiltrating TAMs and the number of LNM (Qing 2012). Additionally, TAMs isolated from M-PTC samples have shown a differential genetic profile when compared with TAMs from NM-PTC samples. Particularly, metastatic TAMs<sup>11</sup> overexpress CXCL8, TGF- $\beta$  and TNF- $\alpha$ , which has been confirmed at proteomic level by measuring these cytokines in conditioned medium (CM) collected from primary TAMs cultures (Fang 2014). This metastatic cytokine profile was not found in PTC cells lines (TPC-1 and B-CPAP), suggesting that, in fact, TAMs could promote the metastatic behaviour of some PTC tumours. Even more, TAMs could train tumour cells to turn into metastatic by a paracrine cytokine-mediated effect, which has been tested by migration assays on PTC cell lines stimulated with or without metastatic TAM-conditioned medium. In this experiment, TPC-1 showed an increased migration and invasion capability in presence of conditioned medium from metastatic TAM, with no effect B-CPAP (Fang 2014).

---

<sup>9</sup> According to this theoretical biological effect of polarised TAMs, M1-TAMs could be classified as pro-oncogenic cells, while M2-TAMs could be classified as pro-metastagenic cells.

<sup>10</sup> Importantly, no previous evidence has described if those TAMs associated with LNM in PTC are more like a M1, or alternatively M2 phenotype.

<sup>11</sup> i.e. TAMs derived from M-PTC primary tumours.

From this previous background, we performed preliminary assays to assess the effect of TNF- $\alpha$  (a metastatic TAM-cytokine, according to the prior results by Fang and colleagues) on the VEGF-R3 pro-metastatic switch as a potential mechanism of how polarised TAM could participate in the LNM development. PTC cell lines were cultured and stimulated with TNF- $\alpha$  for 24 hours (N = 6) to assess the VEGF-R3 and VEGF-C expression. TPC-1 showed an increment of 2.08-fold in VEGF-R3 protein expression compared with the non-stimulated state (control), which was not observed in B-CPAP (figure 6). Furthermore, TNF- $\alpha$  induced a VEGF-C mRNA overexpression in TPC-1 (3.79-fold), with no effect on B-CPAP (figure 7). Together with our previous results, which showed that basal levels of VEGF-R3 and VEGF-C are higher in B-CPAP than TPC-1 (figure 4 and figure 5), these findings suggest that the switch is inducible in non-metastatic cells (TPC-1) by a metastatic TAM-cytokine (TNF- $\alpha$ ), but not in metastatic cells (B-CPAP), since probably the switch has been already activated.

### **1.5 A novel potential mechanism participating on Lymph Node Metastasis development in Papillary Thyroid Cancer**

In brief, the previously discussed background suggests that the VEGF-R3 pro-metastatic switch is observed in samples of M-PTC primary tumour, and specifically at the epithelial cell (i.e. cancer cell) level. Furthermore, evidence shows that those TAMs from M-PTC primary tumours are transcriptomically and secretomically different than those TAMs from NM-PTC primary tumours. And the last, a metastatic TAM-cytokine, TNF- $\alpha$ , induces the VEGF-R3 pro-metastatic switch in a non-metastatic PTC cell line (TPC-1), but not in a metastatic PTC cell line (B-CPAP). Taken together, these results take us to an alternative proposal: a TAM-mediated switch on the VEGF-R3 receptor and ligand profile could be an important mechanism for LNM development in PTC, by inducing pro-metastatic phenotype at the tumour epithelial cell. In this context, this work takes over two emerging questions:

- **Which TAM subtype (M1-like or M2-like cells) induce a VEGF-R3 pro-metastatic switch in PTC?:** the prior evidence suggests that TAMs could participate in the LNM development in PTC, since the grade of TAMs infiltration is associated with LNM, and TNF- $\alpha$  induces an overexpression of VEGF-R3 and VEGF-C in non-metastatic tumour cells. However, it remains unclear the true role of TAMs on inducing that switch observed, and even more, whether those TAMs are M2-like polarised (since M2-TAM are associated with pro-metastatic phenomena) or not.
- **Does the VEGF-R3 pro-metastatic switch activate biological mechanisms that lead to a pro-metastatic phenotype in epithelial tumour cells?:** based on the previous results by Khromova and colleagues (Khromova 2012), we have proposed that VEGF-R3 could play a potential role on the tumour cell transformation toward a more aggressive phenotype in PTC. However, there is no evidence enough to confirm that VEGF-R3 is, at least in part, the signalling pathway responsible for facilitating the pro-metastatic phenotype transformation in epithelial tumour cells (i.e. increasing the EMT, migration capability or invasiveness).

## **2. HYPOTHESIS**

In PTC, M2-TAMs induce a VEGF-R3 pro-metastatic switch at the epithelial tumour cell, promoting the transformation toward a pro-metastatic phenotype.

### 3. OBJECTIVES

#### 3.1 General Objective 1

The first general objective is to study the role of M2-TAMs on inducing the VEGF-R3 pro-metastatic switch in PTC cancer cells. The specific objectives aimed to achieve this are the two described as follow:

##### 3.1.1 Specific Objective 1.1

**To characterise the phenotype and transcriptomic profile of M1-TAMs and M2-TAMs derived from M-PTC and NM-PTC primary tumour samples:** as a first approach, to determine whether infiltrating TAMs within PTC primary tumours were phenotypically more similar to a M1-like or M2-like macrophage, the staining of M1-like and M2-like surface markers (CD80 and CD163, respectively) (Mantovani 2010) were analysed by immunohistochemistry. Then, tumour samples were disaggregated by an enzymatic cocktail into a single cell suspension and sorted by two specific antibodies staining in order to isolate TAMs by their surface marker profile as follow: M1-like cells, defined as CD80(+)/CD163(-); and M2-like cells, defined as CD163(+)/CD80(-). Afterward, to characterise the cytokine transcriptomic profile of sorted cells, Q-PCR assays were performed to assess the genetic expression of different macrophages markers, including M1-TAMs cytokines (IL-6 and IL-12) and M2-TAMs cytokines (IL-1 $\beta$  and IL-10) (Mantovani 2004, Weagen 2015).

##### 3.1.2 Specific Objective 1.2

**To study the effect of TAMs conditioned medium on the VEGF-R3 and VEGF-C expression by epithelial tumour cells:** in order to assess the individual effect of both, M1-TAMs and M2-TAMs in PTC, an *in vitro* model of polarised macrophages was set by stimulating THP-1 cells (undifferentiated monocytes cell line) with specific

cytokine cocktails, according with a previously reported protocol (Genin 2015). To confirm that these *in vitro* differentiated cells showed a similar cytokine transcriptomic profile than those TAMs isolated *ex vivo* (specific objective 1.1), a comparative analysis was performed by Q-PCR. The genetic panel for comparisons included the most relevant M1-TAM cytokines (IL-6 and IL-12) and M2-TAM cytokines (IL-1 $\beta$  and IL-10), according to the characterisation reported by Mantovani and colleagues (Mantovani 2010). Once the *in vitro* model was confirmed to be representative of *ex vivo* TAMs, PTC cell lines (TPC-1 and B-CPAP) were stimulated with conditioned medium from both, M1-THP and M2-THP<sup>12</sup> for 72 hours, in order to assess the response of tumour cells in expressing the VEGF-R3 receptor and secreting VEGF-C. The VEGF-R3 expression was assessed at proteomic level by WB, and the receptor activity (and therefore its functionality) was measured by quantifying pVEGF-R3 (Enzyme-Linked Immunosorbent Assay -ELISA-) after stimulation with VEGF-C. VEGF-C levels were measured in the supernatant by ELISA as well.

## 3.2 General Objective 2

The second general objective is to study the role of the VEGF-R3 pro-metastatic switch in promoting the epithelial tumour EMT and cell migration capability. The specific objectives aimed to achieve this are the two described as follow:

### 3.2.1 Specific Objective 2.1

**To study the role of VEGF-R3 on the PTC cell lines EMT:** PTC cell lines were stimulated with recombinant VEGF-C. After 72 hours, EMT was assessed at phenotype level by microphotography, observing morphological changes associated with EMT (i.e. development of invadopodia and cell size), as well as at genetic level by measuring

---

<sup>12</sup> Polarised macrophages, obtained by the differentiation protocol from THP-1 cells, are named as M1-THP when polarised to a M1-like phenotype, and M2-THP when polarised to a M2-like phenotype.

classical markers of EMT (Snail, Slug and Twist) by Q-PCR. The VEGF-R3 signalling pathway was blocked with a specific kinase inhibitor (MAZ51) (Kirkin 2001) to assess whether EMT triggering was dependent on the receptor activity.

### **3.2.2 Specific Objective 2.2**

**To study the role of VEGF-R3 on the PTC cell lines migration capability:** cell migration assays were performed in order to evaluate the migration capability of PTC cell lines in a Boyden chamber. The cells were previously stimulated with recombinant VEGF-C, blocking or not the VEGF-R3 signalling pathway with the specific kinase inhibitor MAZ51. The bottom chamber was loaded with full culture medium plus serum, while the upper chamber was loaded with culture medium without serum, in order to simulate a nutrient gradient to induce the cell migration. TGF- $\beta$  stimulus was used as a positive control of cell migration inductor (Melzer 2017).

## **4. METHODS**

### **4.1 Patients and Specimens Collection**

Fresh tissue samples from patients with preoperative diagnosis of Bethesda V or Bethesda VI cytology suspicious for PTC (i.e. high probability of malignant nodule) (Cibas 2017) were collected at the surgery room. Patients were enrolled at the Clinical Hospital of the Pontificia Universidad Católica de Chile. Final inclusion criteria were as follows: 18 years or older; cytological suspected diagnosis of PTC; and final surgical pathology confirmation of PTC. Lymph node dissection was performed in those patients with clinical positive lymph nodes by preoperative ultrasound and/or intra-operative pathological findings suggestive of lymph node metastasis. The classification of patients as metastatic or non-metastatic was based on the final pathology report of dissected lymph nodes. All patients signed an informed consent approved by the Ethics Committee of the institution. Tumour samples were immediately placed in a culture medium composed by Dulbecco's Modified Eagle's Medium (DMEM, Sigma-Aldrich) supplemented with 10% fetal bovine serum (FBS, Gibco Invitrogen) and 1% penicillin-streptomycin (100 U/mL, Sigma-Aldrich).

### **4.2 Cell Cultures**

#### **4.2.1 PTC Cell Lines**

PTC cell lines (TPC-1 and B-CPAP) were acquired from the University of Colorado (Denver, US). Cells were cultured by following a lab standardised protocol. Briefly, the culture was performed in a humidified atmosphere containing 5% CO<sub>2</sub> at 37°C, in a culture medium composed by RPMI-1640 Advanced (Gibco Invitrogen) supplemented with 10% FBS, 1% penicillin-streptomycin and L-glutamine 2 mM

(Sigma-Aldrich). The cells were seeded at a density of 500,000 cells/well in 6-well plates (Corning), until a confluency of 80%.

For some assays, cells were pre-incubated in different conditions for 72 hours, previously washed twice with phosphate-buffered saline (PBS, Gibco Invitrogen). The conditions compared for these assays were as follow: negative control (serum-free full medium); CM-M1 (conditioned medium harvested from M1-THP); and CM-M2 (conditioned medium harvested from M2-THP). In particular, for EMT and migration assays, another conditioned was added: TGF- $\beta$  (positive control with Human Recombinant TGF- $\beta$  (PeproTech) in serum-free full medium containing 10 ng/mL of ligand). After each pre-incubation condition, cells were washed twice with PBS.

#### **4.2.2 *In vitro* Macrophages**

THP-1 cell line was used for *in vitro* differentiation of polarised macrophages. Briefly, this monocytic cell line is derived from a 1-year old male diagnosed with Acute Monocytic Leukaemia (Tsuchiya 1980) and has been widely validated as a model of monocyte activity (Lucas 1996, Ollivier 1996) and, under some specific conditions, of Acute Myeloid Leukaemia.

THP-1 monocytes were acquired from the Haemato-Oncology Laboratory of Prof. Bruno Nervi (Pontificia Universidad Católica de Chile, Santiago, Chile). Cells were cultured in DMEM supplemented with 10% FBS and 1% penicillin-streptomycin, in a humidified atmosphere containing 5% CO<sub>2</sub> at 37°C.

An *in vitro* model of polarised macrophages was set by stimulating THP-1 cells with specific cytokine cocktails, according with a previously reported protocol (Genin 2015). In brief, THP-1 monocytes were differentiated into macrophages (M0) by 24-hour incubation with 150 nM phorbol-12-myristate-13-acetate (PMA, Sigma-Aldrich) followed by 24-hour incubation in RPMI-1640 advanced medium (serum-free, in order to avoid any immunoreactivity on macrophages). M0 were polarised into M1-like cells

by incubation with 20 ng/mL of IFN- $\gamma$  (R&D system) and 10 pg/mL of lipopolysaccharide (LPS, Sigma-Aldrich) for 72 hours. M2-like polarisation was obtained by incubation with 20 ng/mL of IL-4 (R&D Systems) and 20 ng/mL of IL-13 (R&D Systems) for 72 hours. THP-1 monocytes were differentiated in 6-well plates.

The polarised macrophages (M1-THP and M2-THP) were grown to a confluency of 60%, washed with PBS, and incubated in serum-free medium for 24 hours. In order to obtain conditioned media from macrophages, the supernatants were harvested, centrifuged 4°C for 5 minutes at 800 RCF to eliminate any detritus, and then passed through a 40  $\mu$ m cell strainer (Cornig).

### **4.3 Immunophenotype characterisation**

#### **4.3.1 Cell Sorting**

After being surgically removed, the management of the surgical piece was performed at sterile conditions. The whole-tissue tumour sample was placed in a 60 mm dish and washed three times with PBS. The sample was carefully cut by using a scalpel in 500  $\mu$ L of PBS, in order to obtain smallest fragments as possible. The homogenised was transferred into a sterile 1.5 mL Eppendorf tube, adding PBS to a final volume of 1 mL. The enzymatic digestion was performed at 37°C for 45 min by adding 90  $\mu$ L of an enzymatic cocktail containing 40  $\mu$ L of Liberase DL 6.5 Wünsch units/mL stock solution (Sigma-Aldrich), 40  $\mu$ L of Liberase TL 13 Wünsch units/mL stock solution (Sigma-Aldrich), and 10  $\mu$ L of DNase-I (New England Biolabs Inc.). The digested suspension was transferred into a sterile 50 mL tube (Falcon) through a 70  $\mu$ m cell strainer (Cornig), assisting the pass through with a gentle flow of PBS supplemented with bovine serum albumin 2% w/v, to a final volume of 20 mL. The suspension was centrifuged at 4°C for 5 minutes at 500 RCF. Finally, the supernatant was discard, and

the pellet suspended in 2 mL of cold DMEM. The single-cell suspension was maintained at 4°C until cell sorting.

After the single-cell suspension was obtained, cells were counted in order to adjust antibodies concentration. The suspension was centrifuged at 4°C for 5 minutes at 500 RCF and re-suspended in 100 µl of PBS with bovine serum albumin 2% w/v per million of cells. Cells were taken to a concentration of 500,000 cells/mL. The cell suspension was incubated with specific antibodies, in concentrations and times according to the manufacturer instructions. Finally, cells were washed and sorted in a BD FACSAria II equipment (BD Biosciences). The first gate was set on FSC/SSC to include the monocyte population. Based on the monocyte gate, double exclusion on FSC-H versus FSC-A was done. From the single cells, the dead cells were excluded by Propidium Iodide staining. Macrophages were divided by gating on CD80 or CD163.

The antibodies used for cell sorting are listed in supplementary content 2.

#### **4.3.2 Immunohistochemistry**

Histological sections were deparaffinised with Histo-Clear (National Diagnostics) and rehydrated through an ethanol gradient. Heat-induced antigen retrieval was performed by immersing slides in Tris-buffered saline containing EDTA (10 mM Tris, 1 mM EDTA, pH 9.0) for 20 minutes at 99°C in a temperature-regulated bath. Endogenous peroxidase activity was suppressed with phosphate-buffered saline containing 3% H<sub>2</sub>O<sub>2</sub> for 20 minutes. In order to prevent non-specific staining, the sample was incubated with a protein solution for 30 minutes, and then incubated with the primary antibody for 45 minutes at room temperature and detected with the VECTA-STAIN Elite ABC Reagent and Vector NovaRED (Vector Laboratories), according to the manufacturer's instructions. Subsequently, sections were rinsed and counterstained with haematoxylin, dehydrated through air exposure and Histo-Clear rinses, and coverslipped.

Digital images were captured using the Aperio AT2 Digital Pathology Scanner (Leica Biosystems). For TAMs staining, the analysis was performed by counting the total cells positive for either, CD80 or CD163, normalised by total tumour cells. Cells were counted in eight random fields at 40X respect to total nuclei. For VEGF-R3, the analysis was performed by considering the intensity of the staining (1, weak; 2, moderate; 3, strong) and the percentage of labelled epithelial tumour cells, in order to calculate the H-Score as described by Pierceall and colleagues (Pierceall 2011).

The antibodies used for IHQ are listed in supplementary content 3.

#### **4.4 Transcriptomic and Proteomic assays**

##### **4.4.1 Real Time Polymerase Chain Reaction (Q-PCR)**

Total RNA was obtained with the RNeasy Plus-Mini Kit (QIAGEN), by following the manufacturer instructions.

RNA concentration was determined using the Epoch<sup>TM</sup> Microplate Spectrophotometer (BioTek). Reverse transcription reaction from 500 ng of total RNA was performed in a final volume of 20 µl using the Improm II<sup>TM</sup> Reverse Transcription System (Promega) following the manufacturer instructions.

For Q-PCR, 10 ng of total RNA from the RT reaction in a final volume of 20 µl were used in the reaction mixture containing 10 µl of 2X Brilliant II SYBR Green qPCR Master-Mix (Agilent), 250 nM of each primer, and nuclease-free water. The Q-PCR reaction was performed in per-sample triplicates in a Rotor-Gene Q cycler (QIAGEN). Thermocycling profile was as follow: 10 min at 95°C, followed by 40 cycles of 20 seconds at 95°C, 20 seconds at 60°C, and 20 seconds at 72°C. Amplicons were subjected to melting curve analysis by increasing the temperature from 72°C to 95°C with an increment of 1°C per second. All reactions with cycle threshold (CT) over 40

and deficient melting curves were not considered for analysis. Two reference genes (GAPDH and PPIA) were used in order to normalize the relative change.

The comparative analysis between two experimental conditions was performed by following the Pfaffl's Method (Pfaffl 2004), according to the international recommendations for Q-PCR analysis. Briefly, let the "Standard" be the reference experimental condition and "Experiment" the condition to be compared with the Standard. For each condition, it was calculated: the CT value of the target gene ( $CT_{target}$ ); and the mean CT value of both reference genes ( $CT_{ref}$ ). Additionally, it was calculated the amplification efficiency of the target gene ( $Eff_{target}$ ); and the amplification efficiency of the reference gene ( $Eff_{ref}$ ). Finally, the relative change of the target in the "Experiment" condition compared to the "Standard" conditioned was calculated as following:

$$Relative\ Change = \frac{Eff_{target}^{(CT_{target\ in\ Experiment}) - (CT_{target\ in\ Standard})}}{Eff_{ref}^{(CT_{ref\ in\ Experiment}) - (CT_{ref\ in\ Standard})}}$$

The primers used for Q-PCR are listed in supplementary content 4.

#### 4.4.2 Western-blotting

Cell specimens were disrupted in protein lysis buffer (Tris-HCl 20 mM pH 7.6, EDTA 1 mM, EGTA 0.5 mM, sucrose 250 mM, triton X-100 1%, Na<sub>4</sub>O<sub>7</sub>P<sub>2</sub> 10 mM, NaF 50 mM, NaVO<sub>3</sub> 1 mM) supplemented with protease inhibitors (Sigma) by intermittent homogenisation on ice. Lysates were centrifuged to collect supernatants. Protein concentration was determined by micro-BCA method (Bio-Rad). Loading samples were prepared by mixing 85 µg of total proteins with LaemmLi's buffer (62.5 µM Tris-HCl, pH 6.8, 10% v/v glycerol, 2.5% w/v SDS, 3% v/v 2-mercaptoethanol, 5% w/v bromophenol blue). Proteins were separated by 7.5% SDS-PAGE and electro-transferred into a nitrocellulose membrane. After 1 hour incubation in 5% non-fat milk-TBS (10 mM Tris-HCl pH 8.0, 150 mM NaCl), the membrane was incubated overnight

at 4°C with primary antibodies. Then, membrane was washed for 5 minutes in TBS-Tween 0.1%, and incubated with HRP-conjugated secondary antibody. SuperSignal™ West Femto Maximum Sensitivity Substrate (Thermo Scientific) was used for protein detection. Membranes were exposed to autoradiography films and manually developed. Protein signal intensity was analysed by densitometry by using the ImageJ version 1.46p software (National Institutes of Health). Densitometry values for target bands were normalised by a load reference ( $\alpha$ -Tubulin).

The antibodies used for WB are listed in supplementary content 5.

#### **4.4.3 Quantification of Soluble Ligand**

PTC cell lines cultured in 6-well plates were grown in different conditions<sup>13</sup> to a confluency of 80%, washed with PBS, and incubated in serum-free medium for 24 hours. The supernatants were harvested, centrifuged 4°C for 5 minutes at 800 RCF to eliminate any detritus, and then passed through a 40  $\mu$ m cell strainer.

Cytokines concentration was determined in per-sample triplicates by the Human VEGF-C Quantikine ELISA Kit (R&D Systems), by following the manufacturer instructions.

#### **4.4.4 Quantification of Phosphorylated Receptor**

PTC cell lines cultured in 6-well plates were grown in different conditions<sup>13</sup> to a confluency of 80%, washed with PBS, and incubated in serum-free medium for 24 hours. Next, for each condition<sup>13</sup>, cells were assigned to 4 treatments in order to measure the specific activation of VEGF-R3 signalling pathway as follow:

---

<sup>13</sup> The conditions compared for these assays were as follow: negative control (serum-free full medium); CM-M1 (conditioned medium harvested from M1-THP); and CM-M2 (conditioned medium harvested from M2-THP).

- Control: no ligand or inhibitor was used; cells were incubated for 140 minutes with serum-free medium.
- MAZ51: cells were incubated for 120 minutes with MAZ51<sup>14</sup> (Calbiochem) in a medium containing 5 nM of inhibitor, and then 20 minutes with serum-free medium.
- VEGF-C: cells were incubated for 120 minutes with serum-free medium, and then 20 minutes with Human Recombinant VEGF-C (PeproTech) in a medium containing 100 ng/mL of ligand.
- MAZ51/VEGF-C: cells were incubated for 120 minutes with MAZ51 in a medium containing 5 nM of inhibitor, and then 20 minutes with Human Recombinant VEGF-C in a medium containing 100 ng/mL of ligand.

After the 140 minutes of treatment, cell specimens were immediately placed on ice and disrupted in protein lysis buffer (Tris-HCl 20 mM pH 7.6, EDTA 1 mM, EGTA 0.5 mM, sucrose 250 mM, triton X-100 1%, Na4O7P2 10 mM, NaF 50 mM, NaVO3 1 mM) supplemented with protease inhibitors by intermittent homogenisation. Lysates were centrifuged to collect supernatants. Protein concentration was determined by micro-BCA method. 50 µg of loading samples were prepared. Phosphorylated VEGF-R3 (pVEGF-R3) concentration was determined in per-sample triplicates by the Human Phospho-VEGFR3/Flt-4 DuoSet IC ELISA kit (R&D Systems), by following the manufacturer instructions.

#### **4.5 Migration assays**

Cell migration was assessed in Boyden chambers (Corning) with 8 µm pore inserts, by culturing cells in a 12-well plate. PTC cell lines were seeded on the inserts and cultured

---

<sup>14</sup> Specific VEGF-R3 tyrosine kinase inhibitor (Kirkin 2001)

for 24 hours at 37°C in the upper chambers with 200 µl of serum-free medium at a density of 50,000 cells/insert. Cells were previously treated in different conditions.

Then, for each condition<sup>15</sup>, cells on the upper surface were assigned to 4 treatments in order to measure the role of VEGF-R3 signalling pathway on migration/invasion as follow:

- Control: no ligand or inhibitor was used; cells were incubated for 24 hours with serum-free medium.
- MAZ51: cells were incubated for 24 hours with MAZ51 in a medium containing 5 nM of inhibitor.
- VEGF-C: cells were incubated for 24 hours with Human Recombinant VEGF-C in a medium containing 100 ng/mL of ligand.
- MAZ51/VEGF-C: cells were incubated for 24 hours with MAZ51 and VEGF-C, in a medium containing 5 nM of inhibitor and 100 ng/mL of ligand.

The bottom chamber was loaded with full medium (serum-enriched) in order to simulate a nutrient gradient to induce the cell migration. Following 24 hours of incubation, cells on the upper surface of Boyden chambers were removed and the cells on the lower surface were stained with 0.01% crystal violet (Sigma Chemical Co.). The membranes were coverslipped and then scanned using the Aperio AT2 Digital Pathology Scanner. Stained cells were counted in four random fields and then expressed as the average number of cells per field.

---

<sup>15</sup> The conditions compared for these assays were as follow: negative control (serum-free full medium); TGF-β (positive control with Human Recombinant TGF-β in serum-free full medium containing 10 ng/mL of ligand); CM-M1 (conditioned medium harvested from M1-THP); and CM-M2 (conditioned medium harvested from M2-THP).

## **4.6 Statistical Analysis**

Statistical tests were two-tailed, and a p-value lower than 0.05 was considered to be statistically significant. Statistical analyses were performed in GraphPad Prism 6 (GraphPad) and SPSS 20.0 (SPSS).

Differences were assessed by non-parametric statistical tests assuming a non-Gaussian distribution of data. The Mann-Whitney U test was used for assessing differences between two independent groups. The Kruskal-Wallis test was used for assessing differences between more than two independent groups.

Experiments involving cell lines by either, cellular, transcriptomic or proteomic measurements, were performed in at least four inter-assay replicates with three intra-assay replicates each one.

Sample size for experiments is detailed on each result and was calculated for statistical accuracy of 95% and statistical power of 80% at least.

## 5. RESULTS

### 5.1 Metastatic PTC tumours show higher infiltration of M2-TAMs and no differences in M1-TAMs compared with non-metastatic tumours

Histological slides from PTC primary tumours were stained for CD80 (M1-like surface marker) and CD163 (M2-like surface marker) by IHQ. Thirty samples of each group (NM-PTC and M-PTC) were analysed by quantifying the proportion of cells with positive staining respect to total tumour cells. A representative image of immunohistochemistry is shown in figure 8.A. M1-TAMs were the most prevalent TAM subtype in both, NM-PTC and M-PTC sample (4.7% M1-TAM versus 0.8% M2-TAM in NM-PTC; 5.4% M1-TAM versus 2.7% M2-TAM in M-PTC). However, the ratio of M1-TAMs respect to M2-TAMs was significantly lower in M-PTC when compared with NM-PTC (2.0 versus 5.9 respectively, p-value 0.0320). Furthermore, M2-TAMs infiltration was significantly higher in M-PTC than NM-PTC (2.7% versus 0.8% respectively, p-value 0.0136), while M1-like macrophages infiltration did not differ between NM-PTC and M-PTC samples (4.7% versus 5.4% respectively, p-value 0.3262) (figure 8.B).

### 5.2 M2-like macrophages isolated from PTC tumours have a differential transcriptomic profile in key cytokines compared with M1-like macrophages

Transcripts of M1-TAM key cytokines (IL-6 and IL-12) and M2-TAM key cytokines (IL-1 $\beta$  and IL-10) were analysed by Q-PCR in TAMs isolated by cell sorting from NM-PTC and M-PTC explants. Four groups were compared (four samples per group): M1-TAMs isolated from NM-PTC (NM-M1); M2-TAMs isolated from NM-PTC (NM-M2); M1-TAMs isolated from M-PTC (M-M1); and M2-TAMs isolated from M-PTC (M-M2). The relative change was calculated as described in methods (see Methods, section 4.4.1),

considering NM-M1 as the “Standard” and each of the other groups as the “Experiment”, wherein the line of no changes was set at 1.

Regarding M1-TAM key cytokines, and compared with NM-M1, IL-6 was similarly expressed in M-M1 (relative change 1.15, p-value 0.4623), but down-expressed in NM-M2 (relative change 0.38, p-value 0.0263) and M-M2 (relative change 0.35, p-value 0.0158) (figure 9.A). Additionally, IL-12 was similarly expressed in M-M1 (relative change 1.06, p-value 0.5012), but down-expressed in NM-M2 (relative change 0.42, p-value 0.0257) and M-M2 (relative change 0.46, p-value 0.0302) (figure 9.B).

Regarding M2-TAM key cytokines, and compared with NM-M1, IL-1 $\beta$  was similarly expressed in M-M1 (relative change 1.07, p-value 0.4788), but overexpressed in NM-M2 (relative change 3.84, p-value 0.0392) and M-M2 (relative change 3.41, p-value 0.0182) (figure 9.C). Additionally, IL-10 was similarly expressed in M-M1 (relative change 1.04, p-value 0.2597), but overexpressed in NM-M2 (relative change 3.95, p-value 0.0352) and M-M2 (relative change 3.40, p-value 0.0451) (figure 9.D).

In summary, for key cytokines (IL-6, IL-12, IL-1 $\beta$  and IL-10), M-M1 showed a similar profile than NM-M1, and M-M2 showed a similar profile than NM-M2. The M2 profile was characterised by an underexpression of M1-TAM key cytokines (IL-6 and IL-12) by approximately 0.4-fold (figure 9.A and figure 9.B), and an overexpression of M2-TAM key cytokines (IL-1 $\beta$  and IL-10) by approximately 4.0-fold (figure 9.C and figure 9.D).

### **5.3 Macrophages polarised *in vitro* display a differential transcriptomic profile in key cytokines comparable to the observed in *ex vivo* TAMs**

Transcripts of M1-TAM key cytokines (IL-6 and IL-12) and M2-TAM key cytokines (IL-1 $\beta$  and IL-10) were analysed by Q-PCR in an *in vitro* model of TAMs polarised from THP-1 cell line, as described in methods (see Methods, section 4.2.2). Three groups were compared (six assays per group): M1-like differentiated cells (M1-THP), M2-like

differentiated cells (M2-THP) and undifferentiated macrophages (M0). Relative change was calculated as described in methods (see Methods, section 4.4.1), considering M0 as the “Standard” and each of the other groups as the “Experiment”, wherein the line of no changes was set at 1.

Representative microphotographs of phenotype changes during the differentiation protocol are shown in figure 10. It is observed that M0 are small, rounded cells, with scarce cytoplasm and few cytoplasmic projections. Once polarised, M1-THP are large, flat cells with scarce cytoplasm but several thin cytoplasmic projections. In contrast, M2-THP are large, rounded cells with a more prominent cytoplasm and some thick cytoplasmic projections. These phenotypes are consistent with morphological characteristics described in previous literature.

Regarding M1-TAM key cytokines, and compared with M0, IL-6 was overexpressed in M1-THP (relative change 4.08, p-value 0.0251) (figure 11.A), but no changes were observed in M2-THP (relative change 0.96, p-value 0.3119) (figure 11.B). Likewise, IL-12 was overexpressed in M1-THP (relative change 4.94, p-value 0.0186) (figure 11.A), with no changes in M2-THP (relative change 1.16, p-value 0.1862) (figure 11.B).

Regarding M2-TAM key cytokines, and compared with M0, IL-1 $\beta$  was overexpressed in M2-THP (relative change 4.97, p-value 0.0023) (figure 11.B), but no changes were observed in M1-THP (relative change 1.04, p-value 0.2312) (figure 11.A). Similarly, IL-10 was overexpressed in M2-THP (relative change 4.12, p-value 0.0213) (figure 11.B), with no changes in M1-THP (relative change 1.19, p-value 0.0900) (figure 11.A).

Therefore, M1-THP were characterised by an overexpression of M1-TAM key cytokines compared to M0, with no significant changes in M2-TAM key cytokines. On the other hand, M2-THP were characterised by an overexpression of M2-TAM key cytokines compared to M0, with no significant changes in M1-TAM cytokines expression (figure 11).

The transcriptomic profile of *in vitro* differentiated TAMs was compared to *ex vivo* isolated TAMs from primary tumours of NM-PTC and M-PTC. For the analysis, NM-M1 was used as the “Standard”. Remarkably, none of the transcriptomic profiles of key cytokines, neither M1 (figure 12.A and figure 12.B) or M2 (figure 12.C and figure 12.D), showed significant differences when comparing M1-like and M2-like cells in NM-PTC, M-PTC and THP-polarised groups. Then, *in vitro* polarised TAMs display a similar transcriptomic profile in key cytokines (IL-6, IL-12, IL-1 $\beta$  and IL-10) compared with *ex vivo* TAMs.

#### **5.4 M2-THP promote the expression of VEGF-R3 in TPC-1 but not in B-CPAP**

The protein expression of VEGF-R3 was measured in TPC-1 and B-CPAP after 72-hour pre-incubation with conditioned medium from *in vitro* differentiated TAM. For each cell line, three groups were compared (six assays per group): FM (cell lines incubated with culture medium only); CM-M1 (cell lines incubated with conditioned medium from M1-THP); and CM-M2 (cell lines incubated with conditioned medium from M2-THP). The relative change in protein expression was calculated respect to TPC-1 pre-incubated with culture medium only.

A representative figure of western-blotting is shown in figure 13.A. In TPC-1, CM-M1 did not induce an increase in VEGF-R3 protein expression (relative change 1.08, p-value 0.6383), but after incubation with CM-M2, VEGF-R3 was overexpressed by 2.48-fold (p-value 0.0368) (figure 13.B). B-CPAP without previous exposure to TAMs conditioned media overexpressed VEGF-R3 by 2.67-fold (p-value 0.0246) respect to TPC-1. Neither CM-M1 or CM-M2 induced changes on VEGF-R3 expression in B-CPAP (p-value 0.2053 and 0.1301, respectively) (figure 13.B). The increase in VEGF-R3 expression in TPC-1 after incubation with CM-M2 was comparable to the VEGF-R3 expression in B-CPAP.

### **5.5 In TPC-1, VEGF-R3 expressed after M2-THP stimulus is biologically active**

The activity of VEGF-R3 was measured in cells pre-incubated for 72 hours with conditioned medium from M1-THP and M2-THP. As described in methods (see Methods, section 4.4.4), four groups were compared per condition (six assays per group): control, MAZ51, VEGF-C and MAZ51/VEGF-C. VEGF-R3 activation was directly measured in cell lysates by quantifying the amount of phosphorylated receptor (pVEGF-R3) by ELISA.

In control, non-stimulated conditions (figure 14.A), VEGF-C induced an increase in pVEGF-R3 on B-CPAP (56 pg versus 32 pg in control, p-value 0.0238), but not on TPC-1 (31 pg versus 24 pg in control, p-value 0.1923). MAZ51 treatment effectively inhibited the increase of pVEGF-R3 induced by VEGF-C in B-CPAP cells (56 pg in VEGF-C stimulus versus 38 pg in MAZ51 treatment before VEGF-C stimulus, p-value 0.0402).

In cells pre-incubated with CM-M1 (figure 14.B), VEGF-C did not induce an increase in pVEGF-R3 on TPC-1 (30 pg versus 26 pg in control, p-value 0.3029), but it did on B-CPAP (60 pg versus 31 pg in control, p-value 0.0399). MAZ51 treatment effectively inhibited the increase of pVEGF-R3 induced by VEGF-C in B-CPAP (60 pg in VEGF-C stimulus versus 33 pg in MAZ51 treatment before VEGF-C stimulus, p-value 0.0289).

In cells pre-incubated with CM-M2 (figure 14.C), VEGF-C induced an increase in pVEGF-R3 on TPC-1 (57 pg versus 29 pg in control, p-value 0.0368), as well as on B-CPAP (62 pg versus 33 pg in control, p-value 0.0219). MAZ51 treatment effectively inhibited the increasing of pVEGF-R3 induced by VEGF-C in TPC-1 (57 pg in VEGF-C stimulus versus 37 pg in MAZ51 treatment before VEGF-C stimulus, p-value 0.0330) and in B-CPAP (62 pg in VEGF-C stimulus versus 43 pg in MAZ51 treatment before VEGF-C stimulus, p-value 0.0418).

Therefore, in TPC-1, pVEGF-R3 was increased in response to VEGF-C stimulus only when cells were pre-incubated with CM-M2, while B-CPAP showed a response to VEGF-C non-dependent to conditioned media from *in vitro* TAMs, neither M1 nor M2.

## **5.6 M2-THP do not promote the secretion of VEGF-C in TPC-1 nor B-CPAP**

To determine whether tumour cells could display autocrine feedback for VEGF-R3 activation, the secretion of VEGF-C was measured in TPC-1 and B-CPAP after 72-hour pre-incubation with conditioned medium from *in vitro* differentiated TAMs (M1-THP and M2-THP). For each cell line, three groups were compared (six assays per group): FM (cell lines incubated with culture medium only); CM-M1 (cell lines incubated with conditioned medium from M1-THP); and CM-M2 (cell lines incubated with conditioned medium from M2-THP). VEGF-C was measured directly in supernatants by quantifying the amount of free ligand by ELISA.

In TPC-1, neither CM-M1 or CM-M2 induced an increased VEGF-C secretion (1512 pg/mL and 1673 pg/mL, p-values 0.3728 and 0.2842, respectively) compared to cells incubated with full culture medium (1430 pg/mL) (figure 15).

Similarly, in B-CPAP, neither CM-M1 or CM-M2 induced an increased VEGF-C secretion (1723 pg/mL and 1691 pg/mL, p-values 0.1992 and 0.3285, respectively) compared to cells incubated with full culture medium (1570 pg/mL) (figure 15).

In basal, non-stimulated conditions, the levels of VEGF-C in supernatants from both, TPC-1 and B-CPAP were similar. Finally, multiple comparison of VEGF-C levels in supernatants of all experimental groups did not show any significant differences (p-value 0.5192 in multiple comparison).

### **5.7 M2-THP secrete significantly more VEGF-C compared with M1-THP and PTC cell lines**

Our results showed that conditioned media from *in vitro* TAMs did not induce VEGF-C secretion by tumour PTC cell lines. Considering that TAMs coexist with tumour cells *in vivo*, the ligand was measured directly in conditioned media from *in vitro* TAMs in order to evaluate a paracrine effect of macrophages in the activation of VEGF-R3 signalling pathway.

In CM-M2, a significantly higher concentration of VEGF-C was detected compared with compared with CM-M1 (27033 pg/mL versus 8591 pg/mL, respectively, p-value 0.0093) (figure 16).

### **5.8 VEGF-C induces morphological changes in TPC-1 pre-incubated with CM-M2 but not in B-CPAP, consistent with a pro-metastatic phenotype**

As a first approach to assess the effect of VEGF-C in inducing a pro-metastatic phenotype, morphological changes were observed in tumour PTC cell lines pre-incubated with conditioned media from *in vitro* TAMs by microscopy. As a positive control, cells were pre-incubated with TGF- $\beta$  in a concentration of 10 ng/mL for 72 hours.

VEGF-C did not induce morphological changes in neither, TPC-1 or B-CPAP when pre-incubated with CM-M1 (data not shown). However, as observed in figure 17, TPC-1 pre-incubated with CM-M2 showed significant changes after 24 hours with VEGF-C (figure top-right), characterised by a lower cell confluence, a prominent, flat cytoplasm and the development of cytoplasmic projections, which is consistent with a stromal-like phenotype observed in B-CPAP (figure bottom-left). These changes were similar to those observed after TGF- $\beta$  pre-incubation (figure top-middle and bottom-middle). VEGF-C did not induce meaningful changes in B-CPAP (figure bottom-right) compared to non-stimulated cell (figure bottom-left).

## **5.9 VEGF-C promotes the expression of EMT genomic regulators in TPC-1 pre-incubated with CM-M2 but not in B-CPAP**

The expression of EMT genomic regulators (Snail, Slug and Twist) was measured by Q-PCR in TPC-1 and B-CPAP, both pre-incubated for 72 hours with conditioned medium from M1-THP and M2-THP. As a positive control, cells were pre-incubated with TGF- $\beta$  in a concentration of 10 ng/mL for 72 hours. As previously described in methods (see Methods, section 4.4.4), four groups were compared per condition (six assays per group): control (no treatment with MAZ51 or VEGF-C), MAZ51 (treatment for 24 hours with MAZ51 but not with VEGF-C), VEGF-C (treatment for 24 hours with VEGF-C but not with MAZ51) and MAZ51/VEGF-C (treatment for 24 hours with VEGF-C and MAZ51). Relative change was calculated as described in methods (see Methods, section 4.4.1), considering TPC-1 pre-incubated with CM-M1 as the “Standard” and each of the other groups as the “Experiment”, wherein the line of no changes was set at 1.

In figure 18 results are shown for Snail. Pre-incubation with positive control TGF- $\beta$  increased expression of Snail in TPC-1 (fourth column in figure 18.A and figure 18.B, relative change 5.97, p-value 0.0185), but there was no effect when cells were pre-incubated with CM-M1, neither in the control (third column in figure 18.A, relative change 1.04, p-value 0.3342) or in VEGF-C group (sixth column in figure 18.A, relative change 1.10, p-value 0.1930). When TPC-1 were pre-incubated with CM-M2, there was an overexpression of Snail (third column in figure 18.B, relative change 2.19, p-value 0.0285) enhanced by VEGF-C treatment (sixth column in figure 18.B, relative change 4.76, p-value 0.0199). On the other hand, B-CPAP overexpressed Snail even when not pre-incubated with CM-M1 or CM-M2 (second column in figure 18.C and figure 18.D, relative change 2.32, p-value 0.0415). TGF- $\beta$  induced an overexpression in B-CPAP (fourth column in figure 18.C and figure 18.D, relative change 5.82, p-value 0.0288). No additional increase in Snail expression was observed in B-CPAP when pre-incubated with CM-M1 (third column in figure 18.C, relative change 2.61, p-value compared to second column 0.4243) or CM-M2 (third column in figure 18.D, relative change 2.38, p-value

compared to second column 0.3844). VEGF-C induced an overexpression of Snail in both, B-CPAP pre-treated with CM-M1 (sixth column in figure 18.C, relative change 4.25, p-value 0.0401) and CM-M2 (sixth column in figure 18.D, relative change 4.19, p-value 0.0396) in similar magnitude. Overall, the VEGF-C treatment effect on Snail expression was effectively inhibited by MAZ51 pre-treatment in both, TPC-1 and B-CPAP.

In figure 19 results are shown for Slug. Similarly, pre-incubation with positive control TGF- $\beta$  induced an overexpression in TPC-1 (fourth column in figure 19.A and figure 19.B, relative change 7.62, p-value 0.0059), but there was no effect when cells were pre-incubated with CM-M1, neither in the control (third column in figure 19.A, relative change 0.97, p-value 0.6294) or in VEGF-C group (sixth column in figure 19.A, relative change 1.06, p-value 0.4091). When TPC-1 were pre-incubated with CM-M2, there was an overexpression of Slug (third column in figure 19.B, relative change 2.34, p-value 0.0460) enhanced by VEGF-C treatment (sixth column in figure 19.B, relative change 3.29, p-value 0.0364). For B-CPAP, Slug was overexpressed even when not pre-incubated with CM-M1 or CM-M2 (second column in figure 19.C and figure 19.D, relative change 2.28, p-value 0.0415). TGF- $\beta$  induced an overexpression in B-CPAP (fourth column in figure 19.C and figure 19.D, relative change 6.35, p-value 0.0029). No further overexpression was observed in B-CPAP when pre-incubated with CM-M1 (third column in figure 19.C, relative change 2.66, p-value compared to second column 0.3003) or CM-M2 (third column in figure 19.D, relative change 2.71, p-value compared to second column 0.1820). VEGF-C induced an overexpression of Slug in both, B-CPAP pre-treated with CM-M1 (sixth column in figure 19.C, relative change 4.37, p-value 0.0235) and CM-M2 (sixth column in figure 19.D, relative change 3.39, p-value 0.0489). Overall, the VEGF-C treatment effect on Slug expression was effectively inhibited by MAZ51 pre-treatment in both, TPC-1 and B-CPAP.

In figure 20 results are shown for Twist. Pre-incubation with positive control TGF- $\beta$  induced an overexpression in TPC-1 (fourth column in figure 20.A and figure 20.B, relative change 5.82, p-value 0.0092), but there was no effect when cells were pre-

incubated with CM-M1, neither in the control (third column in figure 20.A, relative change 1.02, p-value 0.4770) or in VEGF-C group (sixth column in figure 20.A, relative change 1.14, p-value 0.2294). When TPC-1 were pre-incubated with CM-M2, there was an overexpression of Twist (third column in figure 20.B, relative change 2.08, p-value 0.0452) enhanced by VEGF-C treatment (sixth column in figure 20.B, relative change 5.14, p-value 0.0201). B-CPAP overexpressed Twist even when not pre-incubated with CM-M1 or CM-M2 (second column in figure 20.C and figure 20.D, relative change 2.48, p-value 0.0303). TGF- $\beta$  induced an overexpression in B-CPAP (fourth column in figure 20.C and figure 20.D, relative change 5.63, p-value 0.0115). No further overexpression was observed in B-CPAP when pre-incubated with CM-M1 (third column in figure 20.C, relative change 2.53, p-value compared to second column 0.3903) or CM-M2 (third column in figure 20.D, relative change 2.47, p-value compared to second column 0.2038). VEGF-C induced an overexpression of Twist in both, B-CPAP pre-treated with CM-M1 (sixth column in figure 20.C, relative change 3.88, p-value 0.0184) and CM-M2 (sixth column in figure 20.D, relative change 4.98, p-value 0.0298). Overall, the VEGF-C treatment effect on Twist expression was effectively inhibited by MAZ51 pre-treatment in both, TPC-1 and B-CPAP.

In summary, for TPC-1, CM-M1 did not induce any change in classic EMT genomic regulators transcripts (Snail, Slug and Twist), while CM-M2 pre-incubation significantly overexpressed all of them by approximately 2-fold. B-CPAP, independently of the pre-incubation with *in vitro* TAMs conditioned media, already showed a relative overexpression of Snail, Slug and Twist. Only when TPC-1 cells were pre-incubated with CM-M2, VEGF-C induced an overexpression of EMT genomic regulators, which was observed in B-CPAP cells as well.

### **5.10 VEGF-C promotes the migration capability in TPC-1 pre-incubated with CM-M2 but not in B-CPAP**

The migration capability was assessed by a transwell migration assay in TPC-1 and B-CPAP, both pre-incubated for 72 hours with conditioned medium from M1-THP and M2-THP. As a positive control, cells were pre-incubated with TGF- $\beta$  in a concentration of 10 ng/mL for 72 hours. As described in methods (see Methods, section 4.4.4), four groups were compared per condition (six assays per group): control (no treatment with MAZ51 or VEGF-C), MAZ51 (treatment for 24 hours with MAZ51 but not with VEGF-C), VEGF-C (treatment for 24 hours with VEGF-C but not with MAZ51) and MAZ51/VEGF-C (treatment for 24 hours with VEGF-C and MAZ51). The quantification of migrating cells was performed in a Aperio AT2 Digital Pathology Scanner, counting cells in four random fields and then calculating the average number of cells per field.

Without any conditioned medium, B-CPAP migration was significantly higher than TPC-1 (142 versus 58 migrating cells per field, p-value 0.0285). TGF- $\beta$  effectively induced an increased migration in both, TPC-1 (third versus first column in figure 21.A and figure 22.A, 283 versus 58, p-value 0.0058) and B-CPAP (third versus first column in figure 21.B and figure 22.B, 320 versus 142, p-value 0.0192).

TPC-1 cells pre-incubated with CM-M1 did not show an increased migration compared to cells in basal condition (second versus first column in figure 21.A, 70 versus 58, p-value 0.1730). Similarly, B-CPAP pre-incubated with CM-M1 did not show an increased migration compared to cells without pre-incubation (second versus first column in figure 21.B, 169 versus 142, p-value 0.0914). VEGF-C did not induce a higher migration in TPC-1 cells pre-incubated with CM-M1 (fifth versus second column in figure 21.A, 54 versus 70, p-value 0.4902). On the other hand, VEGF-C stimulus increased the migration in B-CPAP pre-incubated with CM-M1 (fifth versus second column in figure 21.B, 281 versus 169, p-value 0.0427).

When TPC-1 cells were pre-incubated with CM-M2, it was an increased migration compared to cells in basal condition (second versus first column in figure 22.A, 110 versus 58, p-value 0.0453). However, as seen with CM-M1, B-CPAP pre-incubated with CM-M2 did not show an increased migration compared to basal conditions (second versus first column in figure 22.B, 103 versus 142, p-value 0.0779). VEGF-C induced a higher migration in TPC-1 cells pre-incubated with CM-M2 (fifth versus second column in figure 22.A, 246 versus 110, p-value 0.0294). Likewise, VEGF-C stimulus increased the migration in B-CPAP pre-incubated with CM-M2 (fifth versus second column in figure 22.B, 271 versus 103, p-value 0.0385).

Therefore, for TPC-1, CM-M1 did not induced any change on migration capability, while CM-M2 pre-incubation significantly increased it. B-CPAP, independently on the pre-incubation with *in vitro* TAMs conditioned media, showed a higher migration compared to TPC-1, but there was no effect of neither, CM-M1 or CM-M2 on it. Only when TPC-1 cells were pre-incubated with CM-M2, VEGF-C induced an increased migration, which was observed on B-CPAP independently of the pre-incubation with CM-M1 or CM-M2.

## 6. DISCUSSION AND CONCLUSIONS

Cancer is a leading public health problem, and it is currently one of the most important topics in clinical and translational research nowadays. The main contributing factor to mortality in cancer patients is the development of LNM, and efforts to unveil the mechanisms underlying this process are continually increasing.

With the intent to improve the clinical outcomes of patients with cancer, we have focused our efforts in elucidating the cellular and molecular mechanisms involved in LNM using PTC as an investigation model. PTC provides excellent model to study early events in LNM development, mainly due to three arguments: i) metastatic spread occurs via lymphatic system in 95% of cases, ii) it is a frequent tumour with a significant number of samples that can be accessed in a wide spectrum of the disease, ranging from non-metastatic to widely invasive tumours, and iii) PTC is a well-differentiated tumour, so it is possible to study early events in the cell transformation from a non-metastatic to a pro-metastatic phenotype.

Previous background suggests that VEGF-R3/VEGF-C system could be an important signalling pathway by which epithelial tumours acquire pro-metastatic characteristics, not only by inducing the development of lymphatic vessels, but also by promoting tumour epithelial cells transformation to a pro-metastatic phenotype. Consistently, our preliminary results have showed increased VEGF-R3 system in samples of M-PTC primary tumour, including an overexpression of both, the receptor and the ligand (figure 2 and figure 3). Moreover, the switch seems to be present specifically at the epithelial cell (i.e. cancer cell) level (figure 4 and figure 5). Therefore, the question arises if this VEGF-R3/VEGF-C expression profile is an active signalling pathway inducing cell changes that will ultimately result in a pro-metastatic phenotype transformation.

Additionally, evidence shows a strong association between TAM infiltration and LNM in PTC, which is consistent with the relevance of the inflammatory microenvironment in the tumour aggressiveness. Then, we initially investigated a possible role of infiltrating TAMs in inducing a VEGF-R3 pro-metastatic switch as a potential mechanism by which TAMs could be involved in the LNM development. As shown, a TAM-derived cytokine, TNF- $\alpha$ , induced an overexpression of both, VEGF-R3 and its ligand VEGF-C, in TPC-1 (non-metastatic PTC cell line) to levels similar to B-CPAP (metastatic PTC cell line) (figure 6 and figure 7). Nonetheless, considering that TAMs are a diverse group of cells with a wide spectrum of polarisation states, we further investigated what TAM subtype (M1-like or M2-like cells) could be responsible for inducing the VEGF-R3 pro-metastatic switch. To our knowledge, no previous studies have reported evidence regarding this question.

Therefore, this research was aimed to answer two questions: which TAM subtype (M1-like or M2-like cells) induce a VEGF-R3 pro-metastatic switch in PTC?; and does the VEGF-R3 pro-metastatic switch activate biological mechanisms that lead to a pro-metastatic phenotype in epithelial tumour cells?

The first general objective took over the first question. Initially, TAM infiltration was studied by IHQ in samples of primary tumours from patients with PTC, excluding aggressive histologies (tall-cell, columnar, diffuse-sclerosing, and poorly differentiated) to avoid potential bias from aggressive subtypes. The percentage of TAM infiltration in PTC was similar to that reported for most of solid tumours, i.e. approximately 5% (Szebeni 2017). Data showed a higher infiltration of M1-TAMs in both, NM-PTC and M-PTC (figure 8). However, the infiltration of M2-TAM was significantly higher in M-PTC. These findings are consistent with the increase of TAM infiltration in PTC reported by Qing and colleagues (Qing 2012), but strongly suggest that increased TAMs in M-PTC could be mostly due to a greater infiltration of M2-like subtype, which is consistent with the theoretical role of M2-like cells as pro-metastagenic (Conway 2016).

To further characterise the infiltrating TAMs from PTC primary tumours, we evaluated the transcriptomic profile of key M1-like (IL-6 and IL-12) and M2-like (IL-1 $\beta$  and IL-10) cytokines, showing that *ex vivo* TAMs with a M1-like Immunophenotype (i.e. positive for CD80 and negative for CD163) in fact overexpressed M1-like cytokines, while *ex vivo* TAMs with a M2-like Immunophenotype (i.e. positive for CD163 and negative for CD80) overexpressed M2-like cytokines (figure 9). Since these cytokines are mediators of most of the functions attributed to M1-like and M2-like TAMs (Rószler 2016), it is reasonable to propose that, at least from a transcriptomic point of view, the polarisation pattern of infiltrating TAMs from PTC primary tumours could be representative of the theoretically expected M1-like and M2-like phenotypes. We are aware that the appropriate experimental approach to confirm this hypothesis would be a wide secretomic profile analysis of isolated TAMs from primary tumours. However, this experiment is technically challenging mainly due to three factors: i) the sorted-cell count needed to obtain a viable primary culture able to secrete measurable cytokines is at least 5,000 cells, which requires a significant amount of tumour tissue; ii) primary tumours obtained from thyroidectomies weigh, in the best of cases, no more than 50 mg, which limits the amount of sorted-cell count; and iii) just few hours after being sorted, macrophages display a large number of phenotypic and transcriptomic changes (Murray 2012), which can disturb the real profile that those TAMs show *in vivo*. For these reasons, we believe that the transcriptomic profiling of *ex vivo* TAMs, immediately after being sorted, is the best possible approach to evaluate the cell polarisation pattern of these infiltrating macrophages.

For similar reasons, the development of a primary cultures from TAMs isolated *ex vivo* by cell sorting in order to obtain conditioned media is difficult to standardise. Therefore, we decided to work with an *in vitro* polarised macrophages model according to a prior protocol reported by Genin and colleagues (Genin 2015). As shown in figures 10, 11 and 12, the phenotypic and transcriptomic characteristic of *in vitro* polarised macrophages is consistent with the characteristics observed in *ex vivo* TAMs, making these cells a valid representation of M1-like and M2-like macrophages that infiltrate PTC primary tumours. Once established, we evaluated the effect of conditioned media from M1-TAMs and M2-

TAMs on the VEGF-R3 pro-metastatic switch. Our findings showed that CM-M2 but not CM-M1 induced an overexpression of VEGF-R3 (figure 13), measured in total cell lysates by WB. This result does not confirm an augmented expression of the receptor at the cell membrane, and further studies such as co-localisation by immunocytochemistry are required. Furthermore, it remains unclear which mechanisms drive an increased VEGF-R3 expression; theoretical alternatives include translational phenomena (i.e. mRNA bioavailability, non-coding RNA enhancing, and increased mRNA translation) and post-translational phenomena (i.e. lower receptor internalisation, higher receptor stability, and increased translocation to cell surface). Another important finding is that the CM-M2 effect was observed only on TPC-1 (a non-metastatic cell line) but not on B-CPAP (a metastatic cell line). This suggests that the switch on VEGF-R3 is inducible before, but not once the tumour cells acquire a metastatic behaviour.

Interestingly, VEGF-R3 expressed in TPC-1 after CM-M2 pre-incubation was biologically active, being activated by VEGF-C (figure 14). From this result, it is possible to propose that the VEGF-R3 overexpression observed in TPC-1 (pre-incubated with CM-M2) is associated with an augmented availability of the receptor at the cell surface. Furthermore, the overexpression of VEGF-R3 should be not only a proteomic switch, but rather a potential source of an increased activation in the signalling pathway dependent on the VEGF-R3/VEGF-C system. Accordingly, we studied the effect of CM-M2 on the VEGF-C expression in PTC cell lines, in order to determine a potential autocrine signalling. Remarkably, none of the conditioned media from neither, M1-TAM or M2-TAM, had any effect on TPC-1 nor B-CPAP, and both cell lines secrete alike amounts of VEGF-C (figure 15), which does not support an autocrine signalling hypothesis. Interestingly, when VEGF-C was measured in CM-M1 and CM-M2, it was found that the concentration of the ligand in conditioned medium from M2-TAM was significantly higher than M1-TAM (figure 16). This suggest that, probably, one of the sources of VEGF-C that could activate the VEGF-R3 signalling pathway are, in fact, M2-TAMs. Although it is not possible to discard that other cells within the tumour microenvironment are secreting VEGF-C, one of the emerging hypothesis is that M2-TAMs can induce the

overexpression of VEGF-R3 in the tumour epithelial cell, while promoting the activation of the signalling pathway by providing the ligand (VEGF-C) in a paracrine way. No previous studies have addressed this hypothesis; however, there is consistent evidence showing that M2-TAMs overexpress VEGF-C, playing an important role in pro-metastatic processes (Kluger 2011, Riabov 2014).

The second general objective took over the second question; considering that M2-TAMs can potentially induce the VEGF-R3/VEGF-C system, we investigated for cellular changes that could explain the effect of an activation of this signalling pathway on the tumour cell transformation toward a pro-metastatic phenotype. This pro-metastatic phenotype was evaluated at three levels: i) morphologic (i.e. changes in the cell surface architecture), ii) transcriptomic (i.e. changes in genomic master regulators of EMT) and iii) functional (i.e. changes in the capability of tumour cells to migrate).

Morphological evaluation showed that, in TPC-1 cells pre-incubated with CM-M2, VEGF-C induced the development of mesenchymal-like structures, such as prominent, flat cytoplasm, cytoplasmic projections, and a lower cell confluence (figure 17). This is consistent with changes observed in cells aimed to migrate and invade beyond the tumour frontier, which basically decrease the mitotic rate to destine the energy expenditure to the cytoskeleton remodelling and cell motion (Hecht 2015). Importantly, regardless the pre-incubation with CM-M1 or CM-M2, pro-metastatic morphological changes occurred in B-CPAP in presence of VEGF-C. Alternatively, for TPC-1 pro-metastatic morphological changes occurred only when previously incubated with CM-M2 followed by VEGF-C, supporting the idea that the pro-metastatic switch is inducible when cells are non-metastatic, and can be further activated in metastatic cells that already have increased VEGF-R3 expression.

Transcriptomically, VEGF-C treatment induced an overexpression of genomic master regulators of EMT (Snail, Slug and Twist) in TPC-1 cells pre-incubated with CM-M2. Moreover, CM-M2 itself induced an overexpression of EMT regulators even when cells

were not treated with VEGF-C (figure 18, figure 19 and figure 20). This result could indicate that, besides the ligand-dependent activation of VEGF-R3 pathway, some cytokines (one or more than one) secreted by M2-TAM could up-regulate the expression of Snail, Slug and Twist. This effect would be not mediated by a ligand-independent activation of VEGF-R3, since MAZ51 alone did not have any effect on EMT regulators expression after pre-incubation with M2-TAM. Once again, independently on the pre-incubation with CM-M1 or CM-M2, B-CPAP responded to VEGF-C treatment, suggesting that the pro-metastatic switch could be already activated in these metastatic cells. Further studies of wide proteomic profiling (e.g. cytokine array) are required in order to determine which M2-TAM cytokines are responsible for inducing the overexpression of EMT regulators. However, good candidates include IL-1 $\beta$  (in colorectal and oral cancer has been associated with ZEB1/Slug/Snail expression, E-cadherin drop, Vimentin expression and increased invasiveness) (Li 2012, Lee 2015) and CCL18 (in ovarian and breast cancer has been associated with E-cadherin drop, Vimentin expression, and migratory/invasive properties) (Su 2014, Wang 2016).

Functionally, TPC-1 cells pre-incubated with CM-M2 increased their migration capability once treated with VEGF-C. As observed by transcriptomic, CM-M2 alone also induced an increased migration, which was enhanced by VEGF-C (figure 21 and figure 22), which is consistent with both, a VEGF-R3-dependent and a VEGF-R3-independent effect mediated by M2-TAMs.

Taken together, the results obtained from this work strongly support the hypothesis that, in PTC, M2-TAMs induce a VEGF-R3 pro-metastatic switch at the epithelial tumour cells, promoting the transformation toward a pro-metastatic phenotype. This study can be considered as an initial step to a rich research pipeline on molecular mechanisms of metastasis, focused on the role of M2-TAMs as a promoter of LNM, and the effect of VEGF-R3 pathway beyond the classic attributed function as pro-lymphangiogenic. Nonetheless, further studies are required to better understand the real meaning of this signalling pathway in the LNM development. As an example, an unanswered question is

which M2-TAM cytokines are regulating the expression of VEGF-R3. Multiplex cytokines array in conditioned medium and multiple knock-down M2-TAM models by CRISPR/Cas9 system could be performed in order to identify the paracrine regulatory mechanism between M2-TAMs and tumour cells. Another important question is which inherent factors, either by the cancer or immune cells, determines that some tumours have an increased M2-TAM infiltration. It is possible that some cancer cells secrete more cytokines favouring M2 polarisation, such as IL-4 and IL-13?, or maybe some patients carry monocytes with an inherited propensity to be polarised to an M2-like phenotype? An interesting study design could be a deep sequencing analysis of tumour cells and peripheral monocytes from patients with non-metastatic disease, to find prognostic factors of LNM development by following-up these patients. In case of finding a prognostic signature in cancer cells, it could be used to predict the risk of development metastasis. Alternatively, if we identified a pre-metastatic peripheral monocytes background to be more liable to turn into M2-like macrophages rather than M1-like, it could be potentially used as a functional assay to predict the personalized risk to develop LNM. Additionally, the VEGF-R3 pro-metastatic switch could be explored for potential using as a biomarker of LNM diagnosis and/or recurrence prediction.

From a therapeutic point of view, the modulation of VEGF-R3 in animal models of PTC is an unexplored option aimed to prevent the development of LNM, or once occurred, to inhibit the progression of the disease.

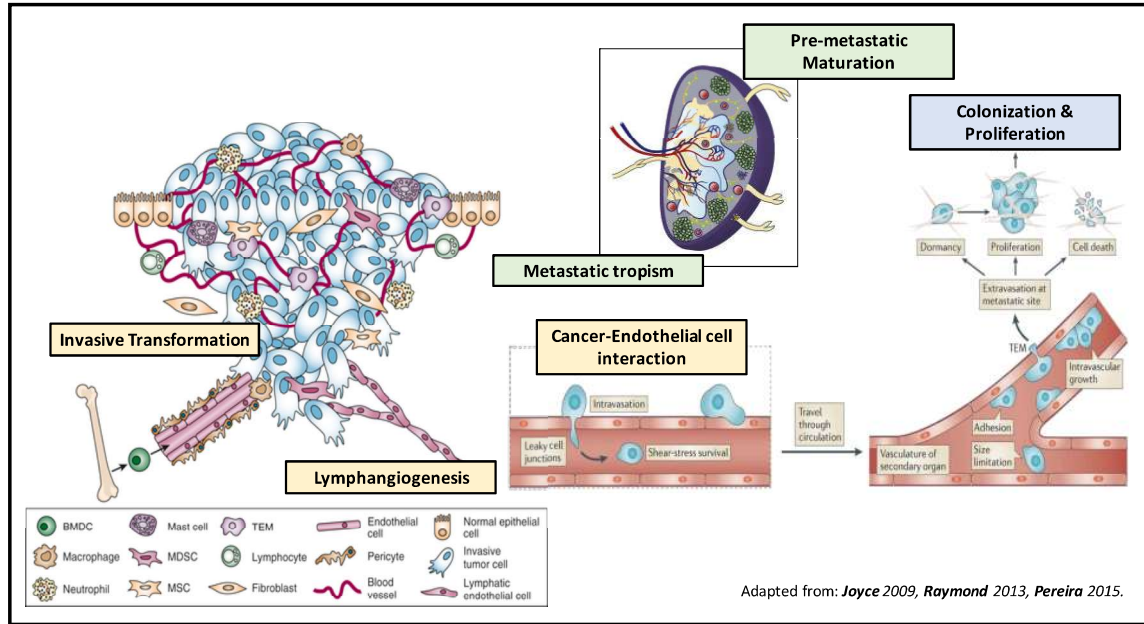
Finally, the same animal models could be used to determine the effect of deviating the polarisation of monocytes from M2-like to an M1-like phenotype. Previously reported evidence suggests a potential role of non-steroidal anti-inflammatory drugs in cancer treatment (Smith 2000, Wang 2003, Harris 2005). Then, it is possible that modulation of M2-TAM-mediated inflammation by targeted therapy could be a future research field aimed to mitigate the risk of LNM development. An emerging alternative includes Dupilumab, a monoclonal antibody that binds to the alpha subunit of the receptor IL-4R $\alpha$ ,

antagonising the signalling pathways of both M2 differentiating cytokines (IL-4 and IL-13) (Wenzel 2013).

We expect that this work can help, in the future, to a better understanding of the mechanisms underlying the LNM development process in PTC, with potential applications in other solid tumours. Ultimately, this could be useful to generate important advances in diagnostic, prognostic and therapeutic tools, with potential impact in thousands of patients with cancer.

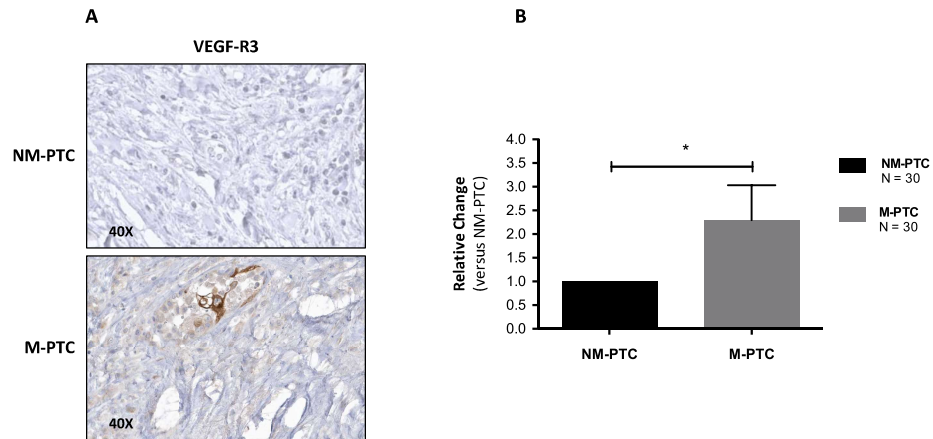
## 7. FIGURES

### 7.1 Figure 1: Schematisation of the LNM development process



The three major components involved on the LNM development are represented. The tumour niche changes (light-yellow boxes) are the invasive transformation of tumour cells, lymphangiogenesis, and cancer-endothelial cell interaction. In the metastatic niche (light-green boxes), changes are summarised in the development of a metastatic tropism, and the pre-metastatic maturation. Finally, the culminant event is the colonisation and proliferation of metastatic tumour cells within the lymph node (light-yellow box).

## 7.2 Figure 2: VEGF-R3 expression in samples of whole-tissue tumour from patients with NM-PTC and M-PTC

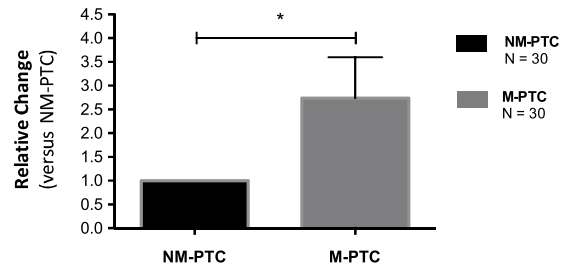


The expression of epithelial VEGF-R3 was assessed by IHQ in 30 samples of whole-tissue tumour from patients with NM-PTC and 30 from M-PTC.

**A.** Representative microphotography of stained slides at 40X optical augmentation. It is observed a higher intensity of VEGF-R3 staining in M-PTC samples.

**B.** Bar plot of relative change on the staining intensity of M-PTC (grey bar) compared to NM-PTC (black bar). The staining intensity was calculated by the H-Score, as described in methods. The staining intensity of VEGF-R3 was 2.38-fold higher in M-PTC (\* p-value 0.0448).

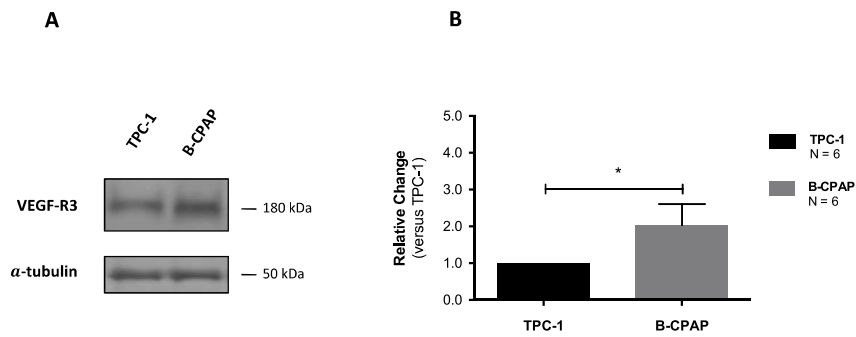
### 7.3 Figure 3: VEGF-C transcript expression in samples of whole-tissue tumour from patients with NM-PTC and M-PTC



The expression of VEGF-C transcript was assessed by Q-PCR in 30 samples of whole-tissue tumour from patients with NM-PTC and 30 from M-PTC. The bar plot shows the relative change on VEGF-C expression using NM-PTC as the Standard, as described in methods.

VEGF-C mRNA level was 2.72-fold higher in M-PTC (grey bar) compared to NM-PTC (black bar) (\* p-value 0.0293).

## 7.4 Figure 4: VEGF-R3 expression in PTC cell lines

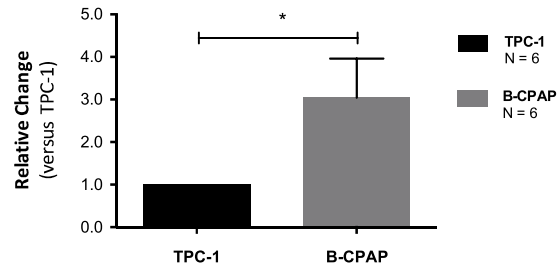


The expression of VEGF-R3 was measured by WB in a cell line model of NM-PTC (TPC-1) and M-PTC (B-CPAP). The average VEGF-R3 expression was calculated from six experiments with three intra-assay replicates.

**A.** Representative western-blot of VEGF-R3 and load reference  $\alpha$ -Tubulin for both cell lines.

**B.** Bar plot of relative change on the VEGF-R3 densitometry respect to TPC-1 (black bar). VEGF-R3 protein level was 2.06-fold higher in B-CPAP (grey bar) (\* p-value 0.0399).

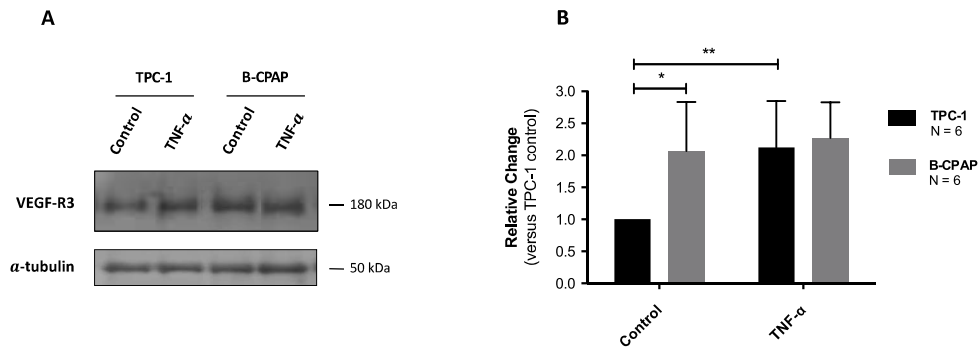
## 7.5 Figure 5: VEGF-C transcript expression in PTC cell lines



The expression of VEGF-C transcript was assessed by Q-PCR in a cell line model of NM-PTC (TPC-1) and M-PTC (B-CPAP). The average VEGF-C transcript expression was calculated from six experiments with three intra-assay replicates. The bar plot shows the relative change on VEGF-C expression using TPC-1 (black bar) as the Standard, as described in methods.

VEGF-C mRNA level was 2.98-fold higher in B-CPAP (grey bar) (\* p-value 0.0205).

## 7.6 Figure 6: VEGF-R3 expression in PTC cell lines after TNF- $\alpha$ stimulus

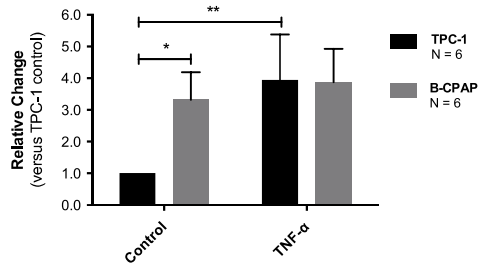


The expression of VEGF-R3 was measured by WB in a cell line model of NM-PTC (TPC-1) and M-PTC (B-CPAP) after being stimulated with TNF- $\alpha$  for 24 hours. The average VEGF-R3 expression was calculated from six experiments with three intra-assay replicates.

**A.** Representative western-blot of VEGF-R3 and load reference  $\alpha$ -Tubulin for both cell lines.

**B.** Bar plot of relative change on the VEGF-R3 densitometry respect to TPC-1 with no TNF- $\alpha$  stimulus (black bar in Control group). The VEGF-R3 protein level in B-CPAP with no TNF- $\alpha$  stimulus (grey bar in Control group) was 1.98-fold higher (\* p-value 0.0371). After incubation with TNF- $\alpha$ , the VEGF-R3 level increased by 2.08-fold in TPC-1 (black bar in TNF- $\alpha$  group) (\*\* p-value 0.0293), while no change was observed in B-CPAP (grey bar in TNF- $\alpha$  group).

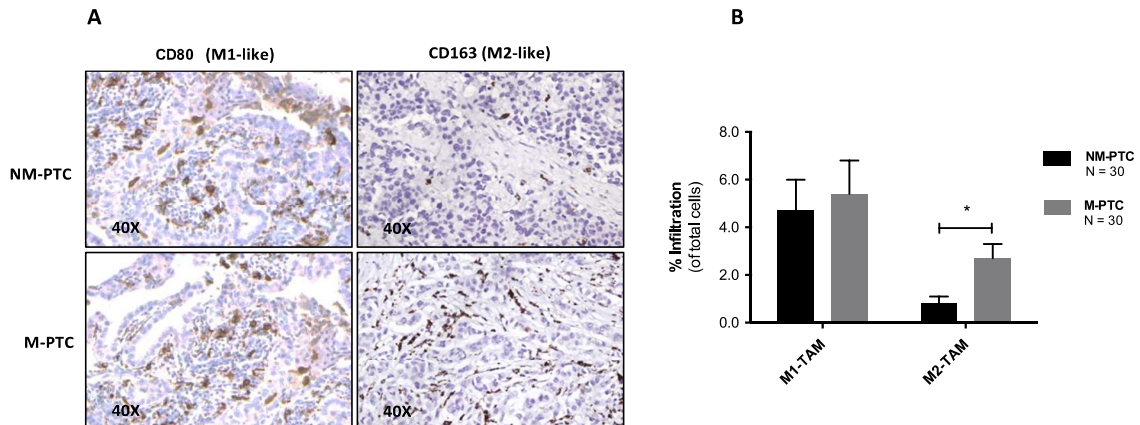
## 7.7 Figure 7: VEGF-C transcript expression in PTC cell lines after TNF- $\alpha$ stimulus



The expression of VEGF-C transcript was assessed by Q-PCR in a cell line model of NM-PTC (TPC-1) and M-PTC (B-CPAP) after being stimulated with TNF- $\alpha$  for 24 hours. The average VEGF-C transcript expression was calculated from six experiments with three intra-assay replicates. The bar plot shows the relative change on VEGF-C expression using TPC-1 with no TNF- $\alpha$  stimulus (black bar in Control group) as the Standard, as described in methods.

VEGF-C mRNA level in B-CPAP with no TNF- $\alpha$  stimulus (grey bar in Control group) was 3.18-fold higher (\* p-value 0.0236). After incubation with TNF- $\alpha$ , the VEGF-R3 level increased by 3.79-fold in TPC-1 (black bar in TNF- $\alpha$  group) (\*\* p-value 0.0395), while no change was observed in B-CPAP (grey bar in TNF- $\alpha$  group).

## 7.8 Figure 8: Infiltration of M1-like and M2-like TAMs in primary tumours from NM-PTC and M-PTC

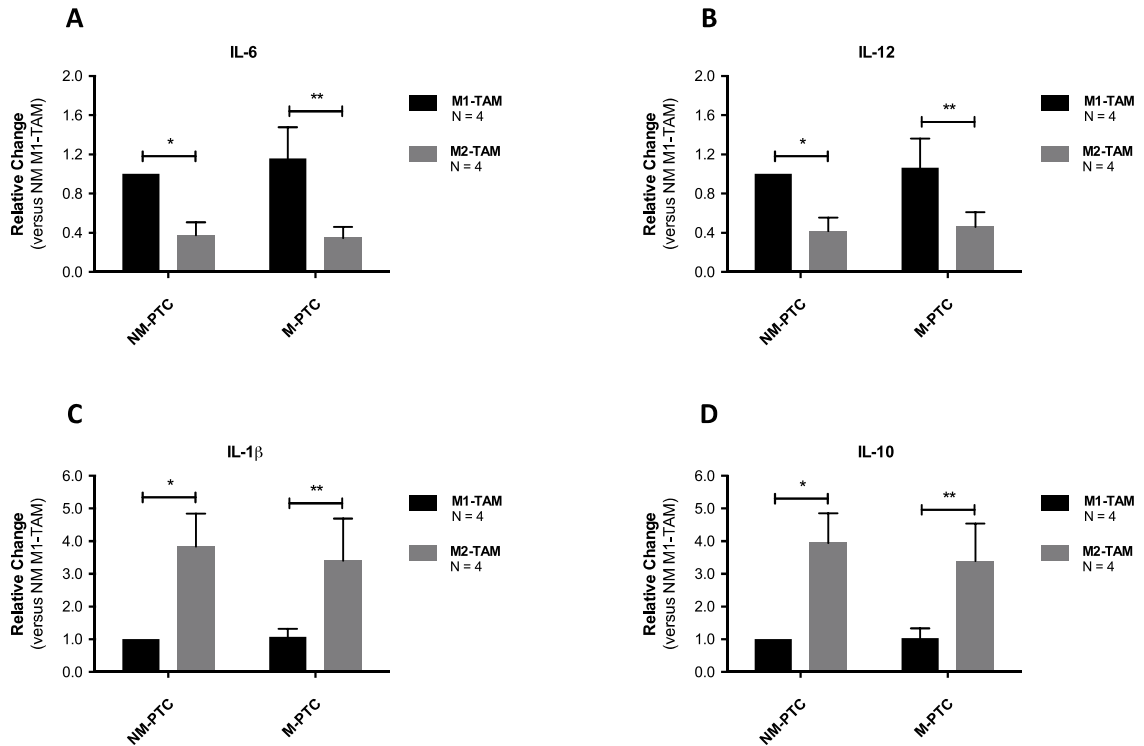


The infiltration of polarised TAMs, either M1-like or M2-like, was assessed by IHQ in samples of primary tumours from patients with NM-PTC and M-PTC, 30 per each. Histological slides were stained for CD80 (M1-like surface marker) and CD163 (M2-like surface marker), quantifying the proportion of cells with positive staining respect to total tumour cells.

**A.** Representative microphotography of stained slides at 40X optical augmentation.

**B.** Bar plot of infiltration percentage of NM-PTC (black bars) and M-PTC (grey bars). M1-TAMs were the most prevalent TAM subtype in both, NM-PTC (4.7%) and M-PTC (5.4%) samples. However, M2-TAMs infiltration was significantly higher in M-PTC than NM-PTC (2.7% versus 0.8% respectively, \* p-value 0.0136), while M1-like macrophages infiltration did not differ between NM-PTC and M-PTC samples (4.7% versus 5.4% respectively, p-value 0.3262). Furthermore, the ratio of M1-TAMs respect to M2-TAMs (M1-TAM/M2-TAM) was significantly lower in M-PTC when compared with NM-PTC (2.0 versus 5.9 respectively, p-value 0.0320).

## 7.9 Figure 9: Transcriptomic profile of key cytokines in TAMs isolated from NM-PTC and M-PTC primary tumours



Transcripts of M1-TAM key cytokines (IL-6 and IL-12) and M2-TAM key cytokines (IL-1 $\beta$  and IL-10) were analysed by Q-PCR in TAMs isolated by cell sorting from NM-PTC (black bars) and M-PTC (grey bars) explants. Average transcript expression was calculated from four experiments with three intra-assay replicates. Relative change was calculated as described in methods, considering M1-TAM from NM-PTC as the Standard.

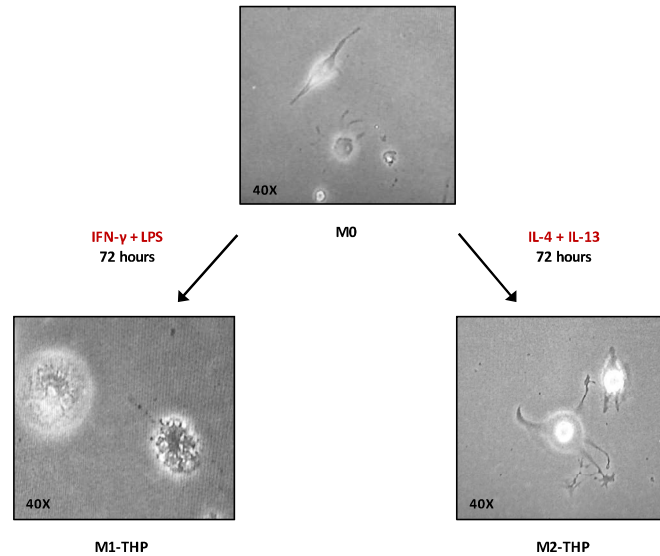
**A.** For IL-6, M2-TAM showed a down-expression in NM-PTC (0.38, \* p-value 0.0263) and M-PTC (0.35, \*\* p-value 0.0158). The expression profile was similar in NM-PTC compared to M-PTC.

**B.** For IL-12, M2-TAM showed a down-expression in NM-PTC (0.42, \* p-value 0.0257) and M-PTC (0.46, \*\* p-value 0.0302). The expression profile was similar in NM-PTC compared to M-PTC.

**C.** For IL-1 $\beta$ , M2-TAM showed an overexpression in NM-PTC (3.84, \* p-value 0.0392) and M-PTC (3.41, \*\* p-value 0.0182). The expression profile was similar in NM-PTC compared to M-PTC.

**D.** For IL-10, M2-TAM showed an overexpression in NM-PTC (3.95, \* p-value 0.0352) and M-PTC (3.40, \*\* p-value 0.0451). The expression profile was similar in NM-PTC compared to M-PTC.

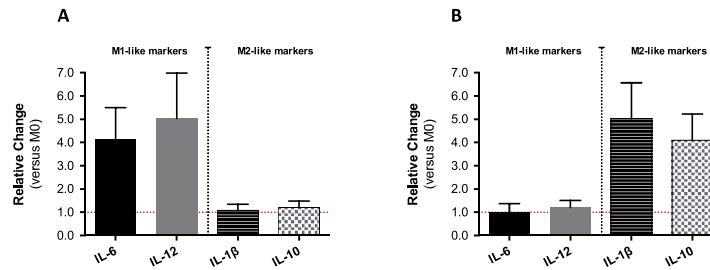
### 7.10 Figure 10: Phenotype changes of *in vitro* polarised macrophages



Representative microphotographs at 40X optical augmentation of phenotype changes during the differentiation protocol of *in vitro* macrophages from THP-1 (monocytes) cells. THP-1 were differentiated into macrophages (M0, top image) by 24-hour incubation with PMA. M0 were polarised into M1-like cells (bottom-left image) by incubation with IFN- $\gamma$  and LPS for 72 hours. M2-like polarisation (bottom-right image) was obtained by incubation with IL-4 and IL-13 for 72 hours.

It is observed that M0 are small, rounded cells, with scarce cytoplasm and few cytoplasmic projections. Once polarized, M1-THP are large, flat cells with scarce cytoplasm but several thin cytoplasmic projections. In contrast, M2-THP are large, rounded cells with a more prominent cytoplasm and some thick cytoplasmic projections.

### 7.11 Figure 11: Transcriptomic profile of key cytokines in TAMs polarised *in vitro* from THP-1 cells

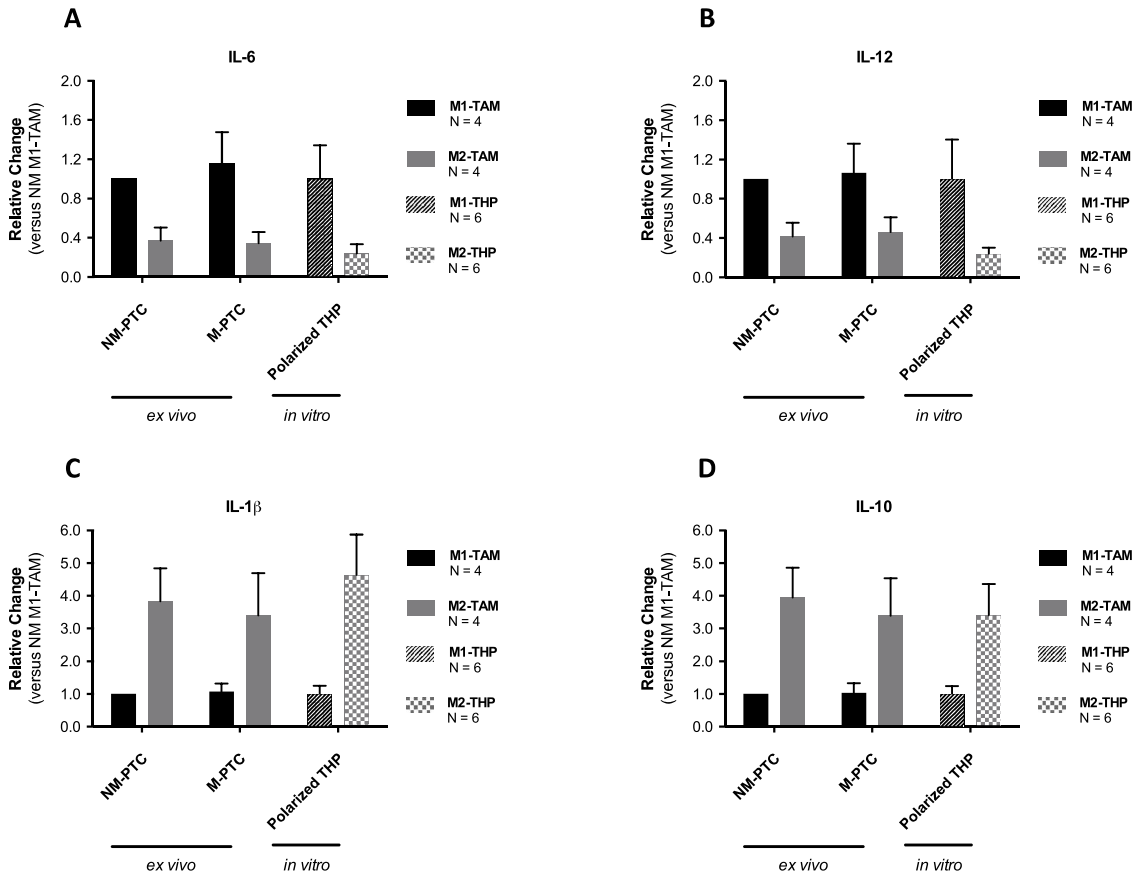


Transcripts of M1-TAM key cytokines (IL-6 in black and IL-12 in grey) and M2-TAM key cytokines (IL-1 $\beta$  in hatched black and IL-10 in hatched white) were analysed by Q-PCR in TAMs polarised *in vitro*. Average transcript expression was calculated from six experiments with three intra-assay replicates. Relative change was calculated as described in methods, considering M0 (i.e. non-polarised macrophages from THP-1 cells previously incubated with PMA) as the Standard.

**A.** M1-THP (i.e. M0 polarised into M1-like cells by incubation with IFN- $\gamma$  and LPS for 72 hours) overexpressed IL-6 (relative change 4.08, p-value 0.0251) and IL-12 (relative change 4.94, p-value 0.0186), with no changes in IL-1 $\beta$  (relative change 1.04, p-value 0.2312) and IL-10 (relative change 1.19, p-value 0.0900).

**B.** M2-THP (i.e. M0 polarised into M2-like cells by incubation with IL-4 and IL-13 for 72 hours) overexpressed IL-1 $\beta$  (relative change 4.97, p-value 0.0023) and IL-10 (relative change 4.12, p-value 0.0213), with no changes in IL-6 (relative change 0.96, p-value 0.3119) and IL-12 (relative change 1.16, p-value 0.1862).

**7.12 Figure 12: Transcriptomic profile of key cytokines in TAMs isolated from PTC primary tumours and TAMs polarised *in vitro* from THP-1 cells**



Transcripts of M1-TAM key cytokines (IL-6 and IL-12) and M2-TAM key cytokines (IL-1β and IL-10) were analysed by Q-PCR in TAMs isolated by cell sorting from NM-PTC and M-PTC explants (*ex vivo* TAMs) and polarised from THP-1 cells (*in vitro* TAMs). Average transcript expression was calculated from four experiments, in case of *ex vivo* TAMs, and six experiments, in case of *in vitro* TAMs, with three intra-assay replicates. Relative change was calculated as described in methods, considering M1-TAM from NM-PTC as the Standard.

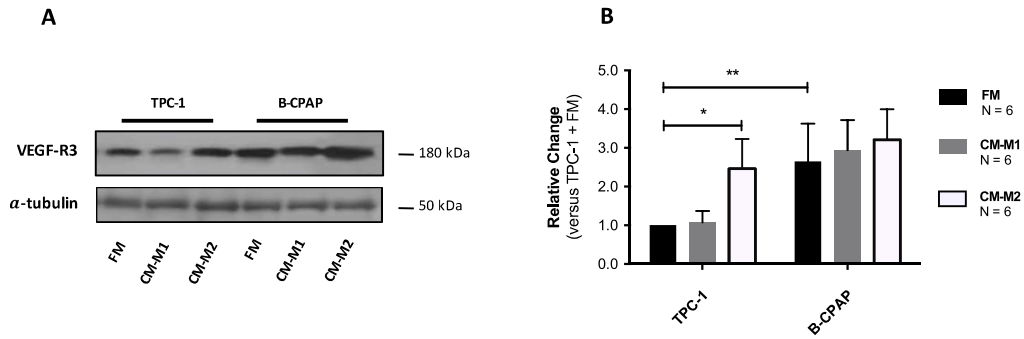
**A.** IL-6 profile was not different when comparing M1-like and M2-like cells in NM-PTC, M-PTC and THP-polarised groups.

**B.** IL-12 profile was not different when comparing M1-like and M2-like cells in NM-PTC, M-PTC and THP-polarised groups.

**C.** IL-1 $\beta$  profile was not different when comparing M1-like and M2-like cells in NM-PTC, M-PTC and THP-polarised groups.

**D.** IL-10 profile was not different when comparing M1-like and M2-like cells in NM-PTC, M-PTC and THP-polarised groups.

### 7.13 Figure 13: Effect of conditioned media from *in vitro* TAMs on VEGF-R3 expression in PTC cell lines

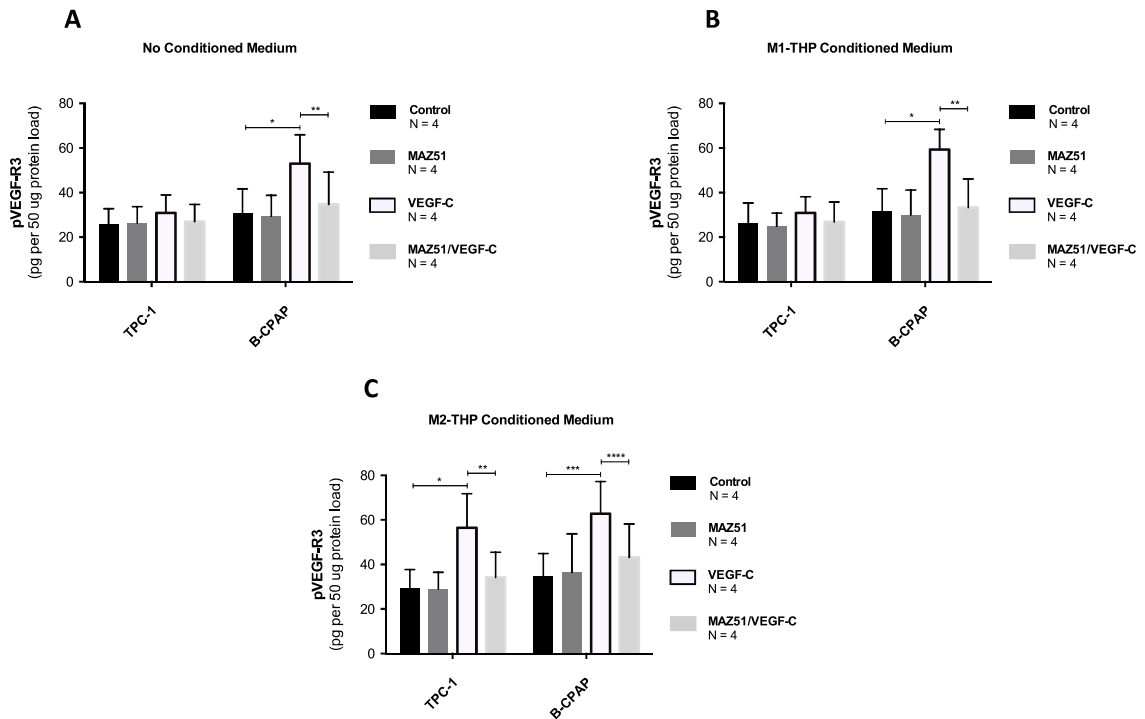


The expression of VEGF-R3 was measured by WB in a cell line model of NM-PTC (TPC-1) and M-PTC (B-CPAP) after being pre-incubated with conditioned medium from *in vitro* polarised TAMs, either M1-like (CM-M1, grey bars) or M2-like (CM-M2, white bars), for 72 hours. The average VEGF-R3 expression was calculated from six experiments with three intra-assay replicates. As a control, cells were pre-incubated with full medium (FM, black bars).

**A.** Representative western-blot of VEGF-R3 and load reference  $\alpha$ -Tubulin for both cell lines.

**B.** Bar plot of relative change on the VEGF-R3 densitometry respect to TPC-1 with no conditioned medium. In TPC-1, CM-M1 did not induce an increase in VEGF-R3 protein expression (1.08, p-value 0.6383), but after incubation with CM-M2, VEGF-R3 was overexpressed by 2.48-fold (\* p-value 0.0368). B-CPAP with no previous exposure to TAMs conditioned media overexpressed VEGF-R3 by 2.67-fold (\*\* p-value 0.0246 compared to TPC-1 + FM). Neither, CM-M1 or CM-M2 induced changes on VEGF-R3 expression in B-CPAP (p-value 0.2053 and 0.1301, respectively).

## 7.14 Figure 14: Activation of VEGF-R3 expressed after incubation with conditioned media from *in vitro* TAMs



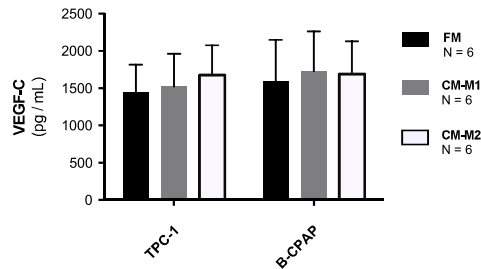
The quantification of phosphorylated VEGF-R3 (pVEGF-R3) was measured by ELISA in a cell line model of NM-PTC (TPC-1) and M-PTC (B-CPAP) after being pre-incubated with conditioned medium from *in vitro* polarised TAMs for 72 hours. The treatments were as follow: control (black bars; cells were incubated for 140 minutes with serum-free medium); MAZ51 (dark-grey bars; cells were incubated for 120 minutes with MAZ51 and then 20 minutes with serum-free medium); VEGF-C (white bars; cells were incubated for 120 minutes with serum-free medium and then 20 minutes with VEGF-C); and MAZ51/VEGF-C (light-grey bars; cells were incubated for 120 minutes with MAZ51 and then 20 minutes with VEGF-C). The average amount of pVEGF-R3 was calculated from six experiments with three intra-assay replicates.

**A.** Without pre-incubation with CM-M1 or CM-M2, VEGF-C did not induce an increase in pVEGF-R3 on TPC-1 (31 pg versus 24 pg in control, p-value 0.1923), but it did on B-CPAP (56 pg versus 32 pg in control, \* p-value 0.0238). MAZ51 effectively inhibited the increasing of pVEGF-R3 induced by VEGF-C in B-CPAP (56 pg in VEGF-C versus 38 pg in MAZ51/VEGF-C, \*\* p-value 0.0402).

**B.** In pre-incubated cells with CM-M1, VEGF-C did not induce an increase in pVEGF-R3 on TPC-1 (30 pg versus 26 pg in control, p-value 0.3029), but it did on B-CPAP (60 pg versus 31 pg in control, \* p-value 0.0399). MAZ51 effectively inhibited the increasing of pVEGF-R3 induced by VEGF-C in B-CPAP (60 pg in VEGF-C versus 33 pg in MAZ51/VEGF-C, \*\* p-value 0.0289).

**C.** In pre-incubated cells with CM-M2, VEGF-C induced an increase in pVEGF-R3 on TPC-1 (57 pg versus 29 pg in control, \* p-value 0.0368), as well as on B-CPAP (62 pg versus 33 pg in control, \*\*\* p-value 0.0219). MAZ51 effectively inhibited the increasing of pVEGF-R3 induced by VEGF-C in TPC-1 (57 pg in VEGF-C versus 37 pg in MAZ51/VEGF-C, \*\* p-value 0.0330) and in B-CPAP (62 pg in VEGF-C versus 43 pg in MAZ51/VEGF-C, \*\*\*\* p-value 0.0418).

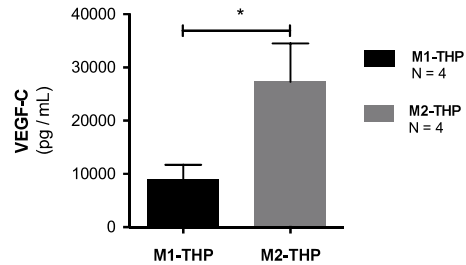
### 7.15 Figure 15: Effect of conditioned media from *in vitro* TAMs on VEGF-C secretion in PTC cell lines



The secretion of VEGF-C was measured by ELISA in a cell line model of NM-PTC (TPC-1) and M-PTC (B-CPAP) after being pre-incubated with conditioned medium from *in vitro* polarised TAMs, either M1-like (CM-M1, grey bars) or M2-like (CM-M2, white bars), for 72 hours. The average VEGF-C concentration was calculated from six experiments with three intra-assay replicates. As a control, cells were pre-incubated with full medium (FM, black bars).

In TPC-1, neither CM-M1 or CM-M2 induced an increased VEGF-C secretion (1512 pg/mL and 1673 pg/mL, p-values 0.3728 and 0.2842, respectively) compared to cells incubated with full culture medium (1430 pg/mL). In B-CPAP, neither CM-M1 or CM-M2 induced an increased VEGF-C secretion (1723 pg/mL and 1691 pg/mL, p-values 0.1992 and 0.3285, respectively) compared to cells incubated with full culture medium (1570 pg/mL). The levels of VEGF-C in supernatants from both, TPC-1 and B-CPAP were similar between them independent on the pre-incubation with either, full medium or conditioned medium from *in vitro* TAMs (p-value 0.5192 in multiple comparison).

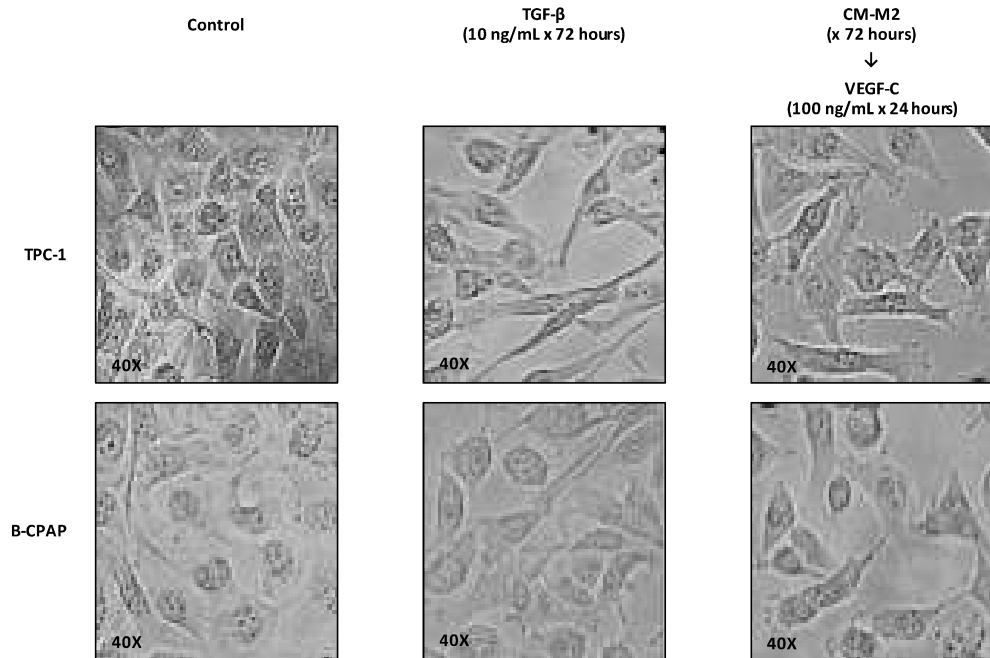
### 7.16 Figure 16: VEGF-C secretion by *in vitro* polarised TAMs



The secretion of VEGF-C was measured by ELISA in TAMs polarised *in vitro*, either M1-like (M1-THP, black bar) or M2-like (M2-THP, grey bar). The average VEGF-C concentration was calculated from four experiments with three intra-assay replicates.

In their supernatants, M2-THP showed a significant higher concentration of VEGF-C compared with M1-THP (27033 pg/mL versus 8591 pg/mL, respectively, \* p-value 0.0093).

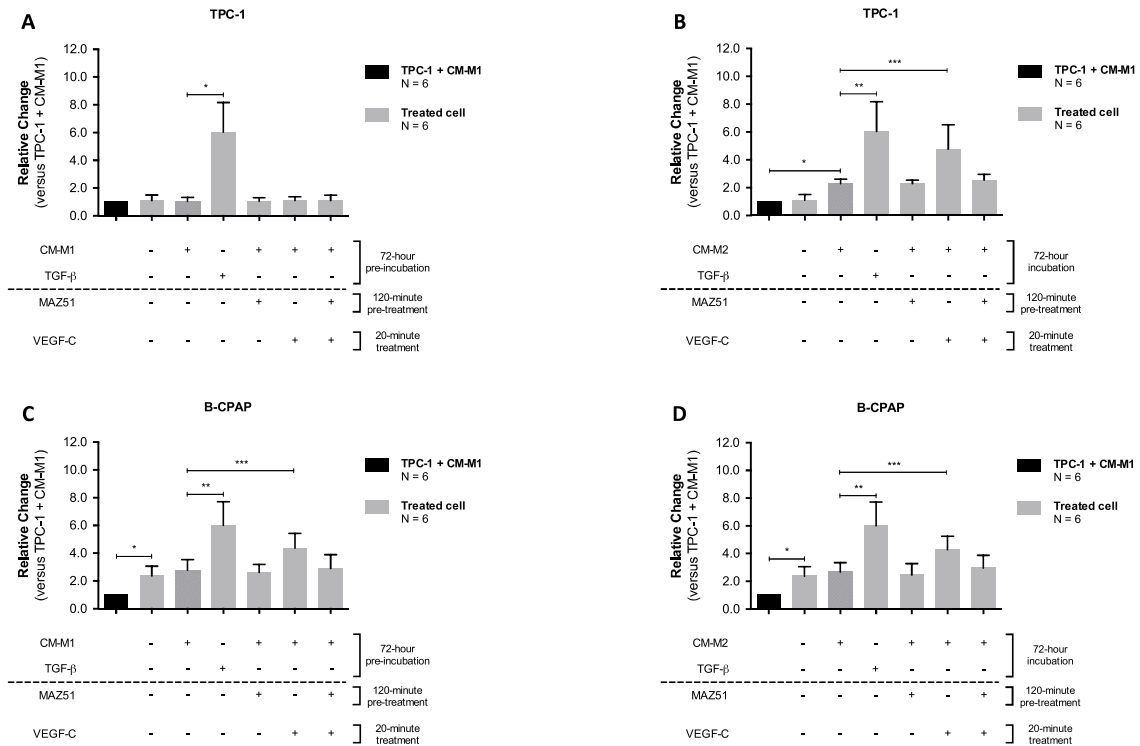
**7.17 Figure 17: Phenotype changes in PTC cell lines after pre-incubation with conditioned medium from M2-THP and treatment with VEGF-C**



Representative microphotographs at 40X optical augmentation of phenotype changes in a cell line model of NM-PTC (TPC-1) and M-PTC (B-CPAP) after being pre-incubated with conditioned medium from M2-THP for 72 hours and then treated with VEGF-C for 24 hours. Pre-incubation with TGF- $\beta$  was used as a positive control for inducing a stromal-like phenotype.

TPC-1 pre-incubated with CM-M2 showed significant changes after 24 hours with VEGF-C (top-right), characterized by a lower cell confluence, a prominent, flat cytoplasm and the development of cytoplasmic projections, which is consistent with a stromal-like phenotype observed in B-CPAP (bottom-left). These changes were similar to those observed after TGF- $\beta$  pre-incubation (top-middle and bottom-middle). VEGF-C did not stimulate remarkable changes in B-CPAP (bottom-right) compared to non-stimulated cell (bottom-left).

### 7.18 Figure 18: Snail transcript expression induced by VEGF-C in PTC cell lines pre-incubated with conditioned media from *in vitro* TAMs



Transcriptomic expression of Snail was analysed by Q-PCR in a cell line model of NM-PTC (TPC-1) and M-PTC (B-CPAP) after being pre-incubated with conditioned medium from *in vitro* polarised TAMs, either M1-like (CM-M1) or M2-like (CM-M2), for 72 hours. Average transcript expression was calculated from six experiments with three intra-assay replicates. Relative change was calculated as described in methods, considering TPC-1 + CM-M1 (black bars) as the Standard, for six different groups (grey bars) as follow: control (cells were pre-incubated with full medium for 96 hours); CM (cells were pre-incubated with conditioned medium for 72 hours, an then 24 hours with neither, MAZ51 or VEGF-C); TGF- $\beta$  (positive control; cells were pre-incubated with TGF- $\beta$  for 72 hours, an then 24 hours with neither, MAZ51 or VEGF-C); MAZ51 (cells were pre-incubated with conditioned medium for 72 hours, an then treated for 24 hours with MAZ51 alone); VEGF-C (cells were pre-incubated with conditioned medium for 72 hours, an then treated for 24 hours with VEGF-C alone); and MAZ51/VEGF-C (cells were pre-incubated with conditioned medium for 72 hours, an then treated for 24 hours with MAZ51 plus VEGF-C).

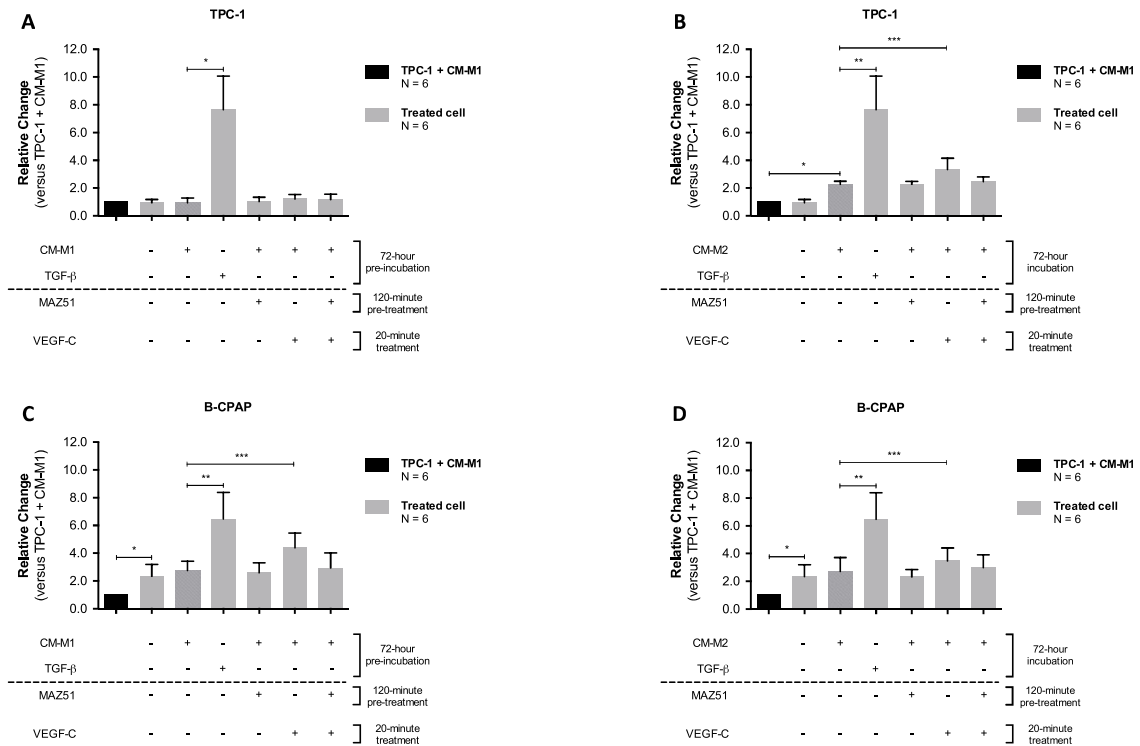
**A. TPC-1 cells pre-incubated with CM-M1.** No effect was observed when cells were pre-incubated with CM-M1, neither alone (relative change 1.04, p-value 0.3342) or treated with VEGF-C (relative change 1.10, p-value 0.1930). TGF- $\beta$  induced an overexpression of Snail (relative change 5.97, \* p-value 0.0185).

**B. TPC-1 cells pre-incubated with CM-M2.** There was an overexpression of Snail when cells were pre-incubated with CM-M2 alone (relative change 2.19, \* p-value 0.0285), further enhanced by the treatment with VEGF-C (relative change 4.76, \*\*\* p-value 0.0199). TGF- $\beta$  induced an overexpression of Snail (relative change 5.97, \*\* p-value 0.0185).

**C. B-CPAP cells pre-incubated with CM-M1.** B-CPAP overexpressed Snail even when not pre-incubated with CM-M1 (relative change 2.32, \* p-value 0.0415). No further effect was observed when cells were pre-incubated with CM-M1 alone (relative change 2.61, p-value 0.4243). Snail expression was increased by VEGF-C (relative change 4.25, \*\*\* p-value 0.0401). TGF- $\beta$  induced an overexpression of Snail (relative change 5.82, p-value \*\* 0.0288).

**D. B-CPAP cells pre-incubated with CM-M2.** B-CPAP overexpressed Snail even when not pre-incubated with CM-M2 (relative change 2.32, \* p-value 0.0415). No further effect was observed when cells were pre-incubated with CM-M2 alone (relative change 2.38, p-value 0.3844). Snail expression was increased by VEGF-C (relative change 4.19, \*\*\* p-value 0.0396). TGF- $\beta$  induced an overexpression of Snail (relative change 5.82, p-value \*\* 0.0288).

### 7.19 Figure 19: Slug transcript expression induced by VEGF-C in PTC cell lines pre-incubated with conditioned media from *in vitro* TAMs



Transcriptomic expression of Slug was analysed by Q-PCR in a cell line model of NM-PTC (TPC-1) and M-PTC (B-CPAP) after being pre-incubated with conditioned medium from *in vitro* polarised TAMs, either M1-like (CM-M1) or M2-like (CM-M2), for 72 hours. Average transcript expression was calculated from six experiments with three intra-assay replicates. Relative change was calculated as described in methods, considering TPC-1 + CM-M1 (black bars) as the Standard, for six different groups (grey bars) as follow: control (cells were pre-incubated with full medium for 96 hours); CM (cells were pre-incubated with conditioned medium for 72 hours, an then 24 hours with neither, MAZ51 or VEGF-C); TGF- $\beta$  (positive control; cells were pre-incubated with TGF- $\beta$  for 72 hours, an then 24 hours with neither, MAZ51 or VEGF-C); MAZ51 (cells were pre-incubated with conditioned medium for 72 hours, an then treated for 24 hours with MAZ51 alone); VEGF-C (cells were pre-incubated with conditioned medium for 72 hours, an then treated for 24 hours with VEGF-C alone); and MAZ51/VEGF-C (cells were pre-incubated with conditioned medium for 72 hours, an then treated for 24 hours with MAZ51 plus VEGF-C).

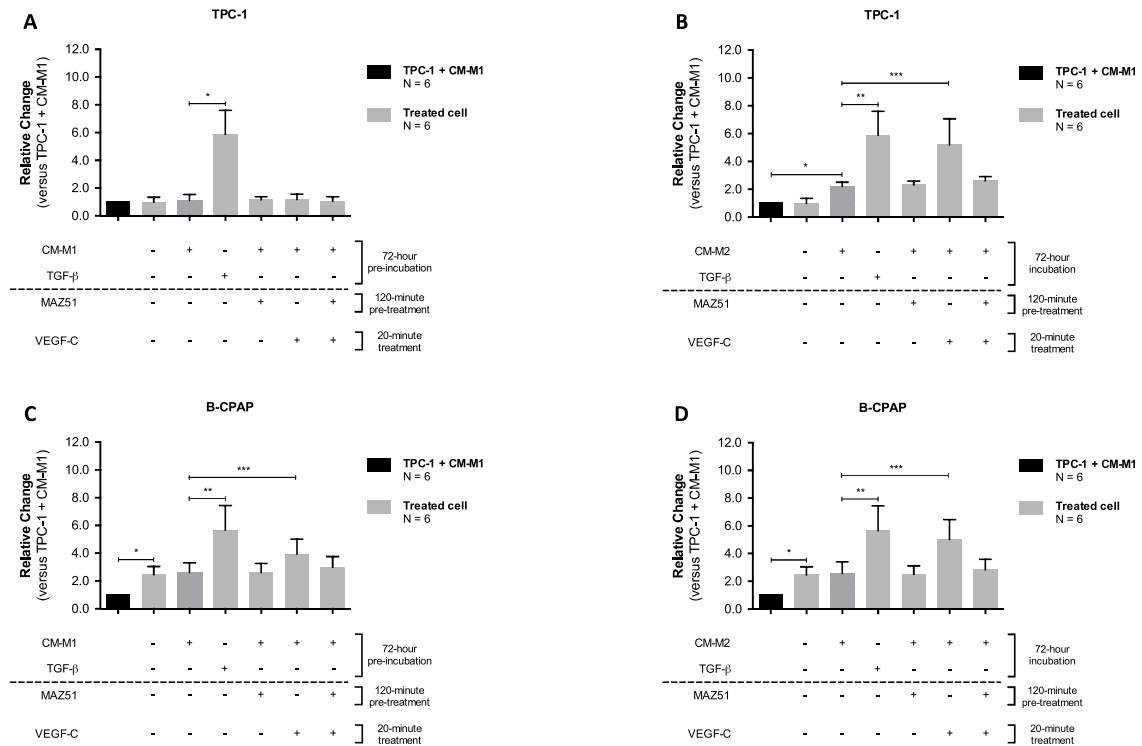
**A. TPC-1 cells pre-incubated with CM-M1.** No effect was observed when cells were pre-incubated with CM-M1, neither alone (relative change 0.97, p-value 0.6294) or treated with VEGF-C (relative change 1.06, p-value 0.4091). TGF- $\beta$  induced an overexpression of Slug (relative change 7.62, \* p-value 0.0059).

**B. TPC-1 cells pre-incubated with CM-M2.** There was an overexpression of Slug when cells were pre-incubated with CM-M2 alone (relative change 2.34, \* p-value 0.0460), further enhanced by the treatment with VEGF-C (relative change 3.29, \*\*\* p-value 0.0364). TGF- $\beta$  induced an overexpression of Slug (relative change 7.62, \* p-value 0.0059).

**C. B-CPAP cells pre-incubated with CM-M1.** B-CPAP overexpressed Slug even when not pre-incubated with CM-M1 (relative change 2.28, \* p-value 0.0415). No further effect was observed when cells were pre-incubated with CM-M1 alone (relative change 2.66, p-value 0.3003). Slug expression was increased by VEGF-C (relative change 4.37, \*\*\* p-value 0.0235). TGF- $\beta$  induced an overexpression of Slug (relative change 6.35, \*\* p-value 0.0029).

**D. B-CPAP cells pre-incubated with CM-M2.** B-CPAP overexpressed Slug even when not pre-incubated with CM-M2 (relative change 2.28, \* p-value 0.0415). No further effect was observed when cells were pre-incubated with CM-M2 alone (relative change 2.71, p-value 0.1820). Slug expression was increased by VEGF-C (relative change 3.39, \*\*\* p-value 0.0489). TGF- $\beta$  induced an overexpression of Slug (relative change 6.35, \*\* p-value 0.0029).

## 7.20 Figure 20: Twist transcript expression induced by VEGF-C in PTC cell lines pre-incubated with conditioned media from *in vitro* TAMs



Transcriptomic expression of Twist was analysed by Q-PCR in a cell line model of NM-PTC (TPC-1) and M-PTC (B-CPAP) after being pre-incubated with conditioned medium from *in vitro* polarised TAMs, either M1-like (CM-M1) or M2-like (CM-M2), for 72 hours. Average transcript expression was calculated from six experiments with three intra-assay replicates. Relative change was calculated as described in methods, considering TPC-1 + CM-M1 (black bars) as the Standard, for six different groups (grey bars) as follow: control (cells were pre-incubated with full medium for 96 hours); CM (cells were pre-incubated with conditioned medium for 72 hours, an then 24 hours with neither, MAZ51 or VEGF-C); TGF-β (positive control; cells were pre-incubated with TGF-β for 72 hours, an then 24 hours with neither, MAZ51 or VEGF-C); MAZ51 (cells were pre-incubated with conditioned medium for 72 hours, an then treated for 24 hours with MAZ51 alone); VEGF-C (cells were pre-incubated with conditioned medium for 72 hours, an then treated for 24 hours with VEGF-C alone); and MAZ51/VEGF-C (cells were pre-incubated with conditioned medium for 72 hours, an then treated for 24 hours with MAZ51 plus VEGF-C).

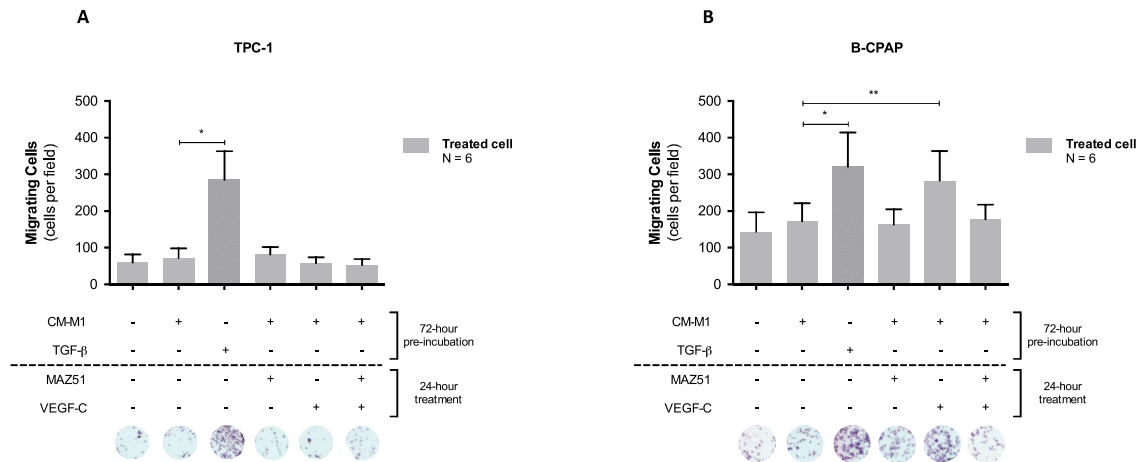
**A. TPC-1 cells pre-incubated with CM-M1.** No effect was observed when cells were pre-incubated with CM-M1, neither alone (relative change 1.02, p-value 0.4770) or treated with VEGF-C (relative change 1.14, p-value 0.2294). TGF- $\beta$  induced an overexpression of Twist (relative change 5.82, \* p-value 0.0092).

**B. TPC-1 cells pre-incubated with CM-M2.** There was an overexpression of Twist when cells were pre-incubated with CM-M2 alone (relative change 2.08, \* p-value 0.0452), further enhanced by the treatment with VEGF-C (relative change 5.14, \*\*\* p-value 0.0201). TGF- $\beta$  induced an overexpression of Twist (relative change 5.97, \*\* p-value 0.0185).

**C. B-CPAP cells pre-incubated with CM-M1.** B-CPAP overexpressed Twist even when not pre-incubated with CM-M1 (relative change 2.48, \* p-value 0.0303). No further effect was observed when cells were pre-incubated with CM-M1 alone (relative change 2.53, p-value 0.3903). Twist expression was increased by VEGF-C (relative change 3.88, \*\*\* p-value 0.0184). TGF- $\beta$  induced an overexpression of Twist (relative change 5.63, \*\* p-value 0.0115).

**D. B-CPAP cells pre-incubated with CM-M2.** B-CPAP overexpressed Twist even when not pre-incubated with CM-M2 (relative change 2.48, \* p-value 0.0303). No further effect was observed when cells were pre-incubated with CM-M2 alone (relative change 2.47, p-value 0.2038). Twist expression was increased by VEGF-C (relative change 4.98, \*\*\* p-value 0.0298). TGF- $\beta$  induced an overexpression of Twist (relative change 5.63, \*\* p-value 0.0115).

**7.21 Figure 21: Effect of VEGF-C on migration capability in PTC cell lines incubated with conditioned medium from M1-THP**



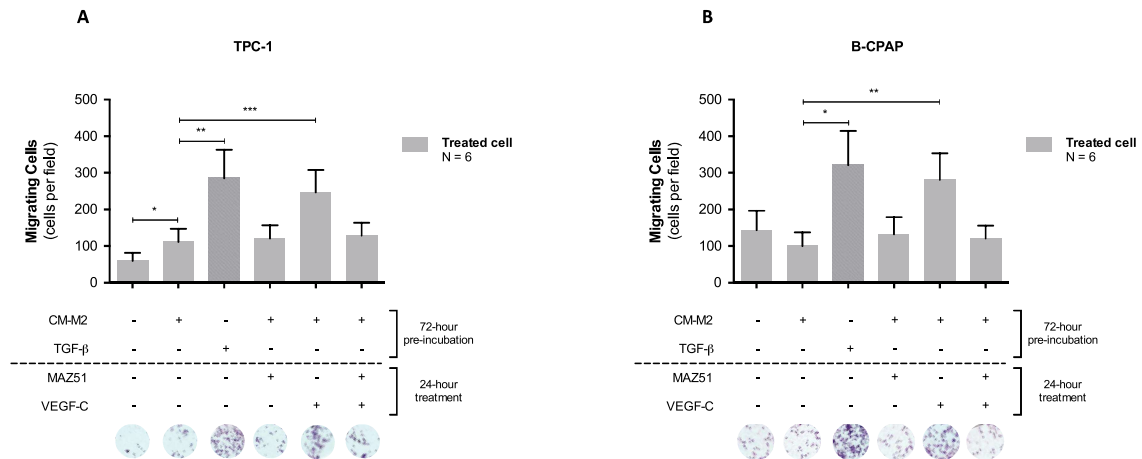
Migration capability was assessed by transwell assays in a cell line model of NM-PTC (TPC-1) and M-PTC (B-CPAP) after being pre-incubated with conditioned medium from M1-THP for 72 hours. Average migration was calculated from six experiments with three intra-assay replicates. Migrating cells were counted in four random fields for six different groups (grey bars) as follow: control (cells were pre-incubated with full medium for 96 hours); CM-M1 (cells were pre-incubated with conditioned medium from M1-THP for 72 hours, an then 24 hours with neither, MAZ51 or VEGF-C); TGF- $\beta$  (positive control; cells were pre-incubated with TGF- $\beta$  for 72 hours, an then 24 hours with neither, MAZ51 or VEGF-C); MAZ51 (cells were pre-incubated with conditioned medium from M1-THP for 72 hours, an then treated for 24 hours with MAZ51 alone); VEGF-C (cells were pre-incubated with conditioned medium from M1-THP for 72 hours, an then treated for 24 hours with VEGF-C alone); and MAZ51/VEGF-C (cells were pre-incubated with conditioned medium from M1-THP for 72 hours, an then treated for 24 hours with MAZ51 plus VEGF-C). Below each bar, a representative microphotograph of the respective stained membrane (with migrating cells) is shown.

**A.** TPC-1 cells pre-incubated with CM-M1 did not show an increased migration compared to control (70 versus 58, p-value 0.1730), and no effect was observed with VEGF-C (54 versus 70 in CM-M1, p-value 0.4902). TGF- $\beta$  effectively induced an increased migration (283 versus 58 in control, \* p-value 0.0058).

**B.** B-CPAP cells pre-incubated with CM-M1 did not show an increased migration compared to control (169 versus 142, p-value 0.0914), but VEGF-C stimulus significantly increased the migrating cells count (281

versus 169 in CM-M1, \*\* p-value 0.0427). TGF- $\beta$  effectively induced an increased migration (320 versus 142 in control, \* p-value 0.0192).

## 7.22 Figure 22: Effect of VEGF-C on migration capability in PTC cell lines incubated with conditioned medium from M2-THP



Migration capability was assessed by transwell assays in a cell line model of NM-PTC (TPC-1) and M-PTC (B-CPAP) after being pre-incubated with conditioned medium from M2-THP for 72 hours. Average migration was calculated from six experiments with three intra-assay replicates. Migrating cells were counted in four random fields for six different groups (grey bars) as follow: control (cells were pre-incubated with full medium for 96 hours); CM-M2 (cells were pre-incubated with conditioned medium from M2-THP for 72 hours, an then 24 hours with neither, MAZ51 or VEGF-C); TGF- $\beta$  (positive control; cells were pre-incubated with TGF- $\beta$  for 72 hours, an then 24 hours with neither, MAZ51 or VEGF-C); MAZ51 (cells were pre-incubated with conditioned medium from M2-THP for 72 hours, an then treated for 24 hours with MAZ51 alone); VEGF-C (cells were pre-incubated with conditioned medium from M2-THP for 72 hours, an then treated for 24 hours with VEGF-C alone); and MAZ51/VEGF-C (cells were pre-incubated with conditioned medium from M2-THP for 72 hours, an then treated for 24 hours with MAZ51 plus VEGF-C). Below each bar, a representative microphotograph of the respective stained membrane (with migrating cells) is shown.

**A.** TPC-1 cells pre-incubated with CM-M2 showed an increased migration compared to control (110 versus 58, \* p-value 0.0453), which was further augmented by VEGF-C (246 versus 110 in CM-M2, \*\*\* p-value 0.0294). TGF- $\beta$  effectively induced an increased migration (283 versus 58 in control, \*\* p-value 0.0058).

**B.** B-CPAP cells pre-incubated with CM-M2 did not show an increased migration compared to control (103 versus 142, p-value 0.0779), but VEGF-C stimulus significantly increased the migrating cells count (271

versus 103 in CM-M2, \*\* p-value 0.0385). TGF- $\beta$  effectively induced an increased migration (320 versus 142 in control, \* p-value 0.0192).

## ABBREVIATIONS

<b>CD</b>	Cluster of Differentiation
<b>CM</b>	Conditioned Medium
<b>CT</b>	Cycling Threshold
<b>DMEM</b>	Dulbecco's Modified Eagle Medium
<b>DNA</b>	Deoxyribonucleic Acid
<b>ECM</b>	Extra-cellular Matrix
<b>EMT</b>	Epithelial-to-Mesenchymal Transition
<b>FBS</b>	Fetal Bovine Serum
<b>GM-CSF</b>	Granulocyte-Macrophage Colony-Stimulating Factor
<b>IFN-<math>\gamma</math></b>	Interferon Gamma
<b>IHQ</b>	Immunohistochemistry
<b>IL</b>	Interleukyn
<b>LNM</b>	Lymph Node Metastasis
<b>M-CSF</b>	Macrophage Colony-Stimulating Factor
<b>M-PTC</b>	Metastatic Papillary Thyroid Cancer
<b>M0</b>	Non-polarised Macrophage derived from THP-1 cell line
<b>M1-TAM</b>	M1-like Tumour Associated Macrophage
<b>M1-THP</b>	Polarised M1-like Macrophage derived from THP-1 cell line
<b>M2-TAM</b>	M2-like Tumour Associated Macrophage
<b>M2-THP</b>	Polarised M2-like Macrophage derived from THP-1 cell line
<b>mRNA</b>	messenger Ribonucleic Acid

<b>MHC</b>	Major Histocompatibility Complex
<b>NM-PTC</b>	Non-Metastatic Papillary Thyroid Cancer
<b>pVEGF-R3</b>	phospho-Vascular Endothelial Growth Factor-Receptor 3
<b>PTC</b>	Papillary Thyroid Cancer
<b>Q-PCR</b>	Quantitative Polymerase Chain Reaction
<b>TAM</b>	Tumour Associated Macrophage
<b>TGF-<math>\beta</math></b>	Transforming Growing Factor Beta
<b>TNF-<math>\alpha</math></b>	Tumour Necrosis Factor Alpha
<b>VEGF-C</b>	Vascular Endothelial Growth Factor-Ligand C
<b>VEGF-R3</b>	Vascular Endothelial Growth Factor-Receptor 3
<b>WB</b>	Western-blotting

## BIBLIOGRAPHY

**Abhinand C, Raju R, Soumya S, et al.** VEGF-A/VEGFR2 signaling network in endothelial cells relevant to angiogenesis. *J Cell Commun Signal.* 2016. Dec;10(4):347-54.

**Ambarus C, Krausz S, van Eijk M, et al.** Systematic validation of specific phenotypic markers for in vitro polarized human macrophages. *J Immunol Methods.* 2012. Jan;375(1-2):196-206.

**Brody T.** Chapter 16 - Oncology Endpoint: Time to Distant Metastasis. In: *Clinical Trials, Second Edition.* Academic Press. 2016.

**Buchheit C, Weigel K, Schafer Z.** Cancer cell survival during detachment from the ECM: multiple barriers to tumour progression. *Nature Publishing Group.* 2014. Sep;14(9):632-41.

**Cao Y.** Opinion: emerging mechanisms of tumour lymphangiogenesis and lymphatic metastasis. *Nat Rev Cancer.* 2005. Sep;5(9):735-43.

**Cibas E, Ali S.** The 2017 Bethesda System for Reporting Thyroid Cytopathology. *Thyroid.* 2017. Nov;27(11):1341-46.

**Conway E, Pikor L, Kung S, et al.** Macrophages, Inflammation, and Lung Cancer. *Am J Respir Crit Care Med.* 2016. Jan;193(2):116-30.

**Davies L, Welch H.** Current thyroid cancer trends in the United States. *JAMA Otolaryngol Head Neck Surg.* 2014. Apr;140(4):317-22.

**Fidler I.** The pathogenesis of cancer metastasis: the “seed and soil” hypothesis revisited. *Nat Rev Cancer.* 2003. Jun;3(6):453-8.

**Fokas E, Engenhardt-Cabillic R, Daniilidis K, et al.** Metastasis: the seed and soil theory gains identity. *Cancer Metastasis Rev.* 2007. Dec;26(3-4):705-15.

**Genin M, Clement F, Fattaccioli A, et al.** M1 and M2 macrophages derived from THP-1 cells differentially modulate the response of cancer cells to etoposide. *BMC Cancer*. 2015. Aug;15:577-91.

**Gress D, Edge S, Greene F, et al.** Part I - Principles of Cancer Staging. In: *AJCC Cancer Staging Manual*, Eighth Edition. American College of Surgeons. 2018.

**Hanahan D, Folkman J.** Patterns and emerging mechanisms of the angiogenic switch during tumorigenesis. *Cell*. 1996. Aug;86(3):353-64.

**Harris R, Beebe-Donk J, Doss H, et al.** Aspirin, ibuprofen, and other non-steroidal anti-inflammatory drugs in cancer prevention: a critical review of non-selective COX-2 blockade (review). *Oncol Rep*. 2005. Apr;13(4):559-83.

**Hecht I, Natan S, Zaritsky A, et al.** The motility-proliferation-metabolism interplay during metastatic invasion. *Sci Rep*. 2015. Sep;5(1):13538-48.

**Joyce J, Pollard J.** Microenvironmental regulation of metastasis. *Nat Rev Cancer*. 2009. Apr;9(4):239-52.

**Keen J, Moore H.** The Genotype-Tissue Expression (GTEx) Project: Linking Clinical Data with Molecular Analysis to Advance Personalized Medicine. *Journal of Personalized Medicine*. 2015. Dec;5(4):22-9.

**Khromova N, Kopnin P, Rybko V, et al.** Downregulation of VEGF-C expression in lung and colon cancer cells decelerates tumor growth and inhibits metastasis via multiple mechanisms. *Oncogene*. 2012. Mar;31(11):1389-97.

**Kirkin V, Mazitschek R, Krishnan J, et al.** Characterization of indolinones which preferentially inhibit VEGF-C- and VEGF-D-induced activation of VEGFR-3 rather than VEGFR-2. *Eur J Biochem*. 2001. Nov;268(21):5530-40.

**Kluger M, Colegio O.** Lymphangiogenesis linked to VEGF-C from tumor-associated macrophages: accomplices to metastasis by cutaneous squamous cell carcinoma?. *J Invest Dermatol*. 2011. Jan;131(1):17-19.

- Lee C, Chang J, Syu S, et al.** IL-1 $\beta$  promotes malignant transformation and tumor aggressiveness in oral cancer. *J Cell Physiol.* 2015. Apr;230(4):875-84.
- Li Y, Wang L, Pappan L, et al.** IL-1 $\beta$  promotes stemness and invasiveness of colon cancer cells through Zeb1 activation. *Mol Cancer.* 2012. Nov;11:87-100.
- Lucas M, Mazzone T.** Cell surface proteoglycans modulate net synthesis and secretion of macrophage apolipoprotein E. *J Biol Chem.* 1996. Jun;271(23):13454-60.
- Mantovani A, Sica A.** Macrophages, innate immunity and cancer: balance, tolerance, and diversity. *Curr Opin Immunol.* 2010. Apr;22(2):231-7.
- Mantovani A, Sica A, Sozzani S, et al.** The chemokine system in diverse forms of macrophage activation and polarization. *Trends Immunol.* 2004. Dec;25(12):677-86.
- Mantovani A, Sozzani S, Locati M, et al.** Macrophage polarization: tumor-associated macrophages as a paradigm for polarized M2 mononuclear phagocytes. *Trends Immunol.* 2002. Nov;23(11):549-55.
- Massagué J, Obenauf AC.** Metastatic colonization by circulating tumour cells. *Nature.* 2016. Jan;529(7586):298-306.
- Melzer C, von der Ohe J, Hass R, et al.** TGF- $\beta$ -Dependent Growth Arrest and Cell Migration in Benign and Malignant Breast Epithelial Cells Are Antagonistically Controlled by Rac1 and Rac1b. *Int J Mol Sci.* 2017. Jul;18(7):1574-90.
- Morris L, Tuttle R, Davies L.** Changing Trends in the Incidence of Thyroid Cancer in the United States. *JAMA Otolaryngol Head Neck Surg.* 2016. Jul;142(7):709-11.
- Mosser D, Edwards J.** Exploring the full spectrum of macrophage activation. *Nat Rev Immunol.* 2008. Dec;8(12):958-69.
- Nguyen D, Bos P, Massagué J.** Metastasis: from dissemination to organ-specific colonization. *Nature Publishing Group.* 2009. Apr;9(4):274-84.
- Noguchi S, Noguchi A, Murakami N.** Papillary carcinoma of the thyroid. I. Developing pattern of metastasis. *Cancer.* 1970. Nov;26(5):1053-60.

**McColl B, Loughran S, Davydova N, et al.** Mechanisms of lymphangiogenesis: targets for blocking the metastatic spread of cancer. *Curr Cancer Drug Targets*. 2005. Dec;5(8):561-71.

**Murray P, Wynn T.** Protective and pathogenic functions of macrophage subsets. *Nat Rev Immunol*. 2011. Aug;11(11):723-37.

**Ollivier V, Parry G, Cobb R, et al.** Elevated cyclic AMP inhibits NF-kappaB-mediated transcription in human monocytic cells and endothelial cells. *J Biol Chem*. 1996. Aug;271(34):20828-35.

**Pellegriti G, Frasca F, Regalbuto C, et al.** Worldwide increasing incidence of thyroid cancer: update on epidemiology and risk factors. *J Cancer Epidemiol*. 2013. 2013(1):965212-22.

**Pereira E, Jones D, Jung K, et al.** The lymph node microenvironment and its role in the progression of metastatic cancer. *Semin Cell Dev Biol*. 2015. Feb;38(1):98-105.

**Pfaffl M.** Chapter 3 - Quantification strategies in real-time PCR. In: *A-Z of quantitative PCR*, First Edition. International University Line. 2004.

**Pierceall W, Wolfe M, Suschak J, et al.** Strategies for H-score normalization of preanalytical technical variables with potential utility to immunohistochemical-based biomarker quantitation in therapeutic response diagnostics. *Anal Cell Pathol*. 2011. Jun;34(3):159-68.

**Polyak K, Weinberg R.** Transitions between epithelial and mesenchymal states: acquisition of malignant and stem cell traits. *Nature Publishing Group*. 2009. Apr;9(4):265-73.

**Rahib L, Smith B, Aizenberg R, et al.** Projecting Cancer Incidence and Deaths to 2030: The Unexpected Burden of Thyroid, Liver, and Pancreas Cancers in the United States. *Cancer Research*. 2014. May;74(11):2913-21.

**Relf M, LeJeune S, Scott P, et al.** Expression of the angiogenic factors vascular endothelial cell growth factor, acidic and basic fibroblast growth factor, tumor growth

factor beta-1, platelet-derived endothelial cell growth factor, placenta growth factor, and pleiotrophin in human primary breast cancer and its relation to angiogenesis. *Cancer Research*. 1997. Mar;57(5):963-9.

**Reymond N, d'Água B, Ridley A.** Crossing the endothelial barrier during metastasis. *Nat Rev Cancer*. 2013. Dec;13(12):858-70.

**Riabov V, Gudima A, Wang N, et al.** Role of tumor associated macrophages in tumor angiogenesis and lymphangiogenesis. *Front Physiol*. 2014. Mar;5(1):75-88.

**Ribeiro F, Meireles A, Rocha A, et al.** Conventional and molecular cytogenetics of human non-medullary thyroid carcinoma: characterization of eight cell line models and review of the literature on clinical samples. *BMC Cancer*. 2008. Dec;8(1):371-82.

**Röszer T.** Understanding the Mysterious M2 Macrophage through Activation Markers and Effector Mechanisms. *Mediators Inflamm*. 2015. May;2015(1):816460-76.

**Saharinen P, Tammela T, Karkkainen M, et al.** Lymphatic vasculature: development, molecular regulation and role in tumor metastasis and inflammation. *Trends Immunol*. 2004. Jul;25(7):387-95.

**Saiselet M, Floor S, Tarabichi M, et al.** Thyroid cancer cell lines: an overview. *Front Endocrinol*. 2012. Nov;3(1):133-42.

**Siegel R, Miller K, Jemal A.** Cancer statistics, 2016. *CA Cancer J Clin*. 2016. Jan;66(1):7-30.

**Simpson C, Anyiwe K, Schimmer A.** Anoikis resistance and tumor metastasis. *Cancer Letters*. 2008. Dec;272(2):177-85.

**Sleeman J, Thiele W.** Tumor metastasis and the lymphatic vasculature. *Int J Cancer*. 2009. Dec;125(12):2747-56.

**Smith M, Hawcroft G, Hull M.** The effect of non-steroidal anti-inflammatory drugs on human colorectal cancer cells: evidence of different mechanisms of action. *Eur J Cancer*. 2000. Mar;36(5):664-74.

**Su S, Liu Q, Chen J, et al.** A positive feedback loop between mesenchymal-like cancer cells and macrophages is essential to breast cancer metastasis. *Cancer Cell*. 2014. May;25(5):605-20.

**Szebeni G, Vizler C, Kitajka K, et al.** Inflammation and Cancer: Extra- and Intracellular Determinants of Tumor-Associated Macrophages as Tumor Promoters. *Mediators Inflamm*. 2017. Jan;2017(1):9294018-31.

**Thiery J, Sleeman J.** Complex networks orchestrate epithelial-mesenchymal transitions. *Nat Rev Mol Cell Biol*. 2006. Feb;7(2):131-42.

**Tsuchiya S, Yamabe M, Yamaguchi Y, et al.** Establishment and characterization of a human acute monocytic leukemia cell line (THP-1). *Int J Cancer*. 1980. Aug;26(2):171-76.

**Uhlén M, Fagerberg L, Hallström B, et al.** Proteomics. Tissue-based map of the human proteome. *Science*. 2015. Jan;347(6220):126041-9.

**Wang Q, Tang Y, Yu H, et al.** CCL18 from tumor-cells promotes epithelial ovarian cancer metastasis via mTOR signaling pathway. *Mol Carcinog*. 2016. Nov;55(11):1688-99.

**Wang W, Huang J, Zheng G, et al.** Non-steroidal anti-inflammatory drug use and the risk of gastric cancer: a systematic review and meta-analysis. *J Natl Cancer Inst*. 2003. Dec;95(23):1784-91.

**Wartofsky L, Van Nostrand D.** Chapter 2 - The Thyroid Gland: The Basics. In: *Thyroid Cancer*, Second Edition. Keystone Press. 2010.

**Weigel E, Smith C, Ping Guo L, et al.** Macrophage Polarization and Its Role in Cancer. *Journal of Clinical & Cellular Immunology*. 2015. Jan;06(04):1-8.

**Wenzel S, Ford L, Pearlman D, et al.** Dupilumab in persistent asthma with elevated eosinophil levels. *N Engl J Med*. 2013. Jun;368(26):2455-66.

**Whiteside T.** The tumor microenvironment and its role in promoting tumor growth. *Oncogene*. 2008. Jun;27(45):5904-12.

**Wong S, Hynes R.** Lymphatic or hematogenous dissemination: how does a metastatic tumor cell decide?. *Cell Cycle*. 2006. May;5(8):812-7.

**World Health Organization.** Fact Sheets on Cancer. In: <https://www.who.int/news-room/fact-sheets/detail/cancer>. 2018.

**Zhang L, Zhou F, Han W, et al.** VEGFR-3 ligand-binding and kinase activity are required for lymphangiogenesis but not for angiogenesis. *Cell Res*. 2010. Aug;20:1319-31.

**Zhang S, Yi S, Zhang D. et al.** Intratumoral and peritumoral lymphatic vessel density both correlate with lymph node metastasis in breast cancer. *Sci Rep*. 2017. Jan;7(1):40364-71.

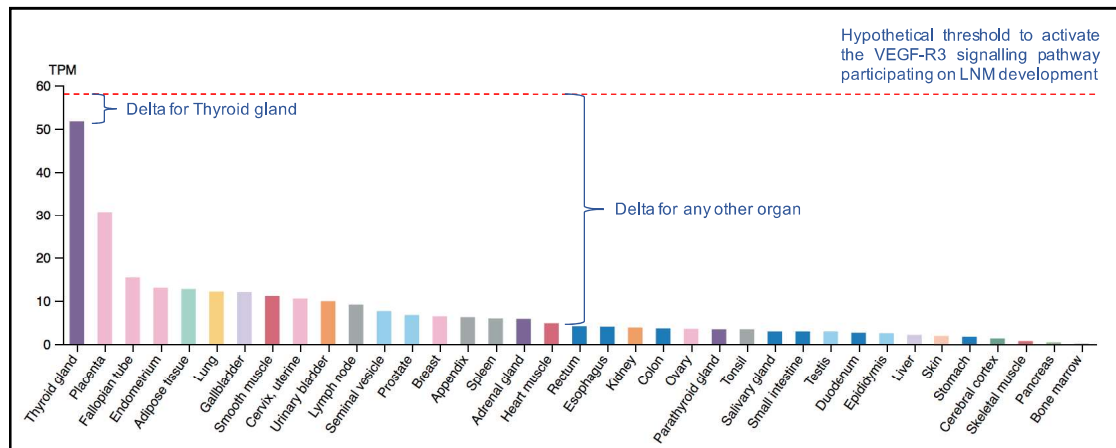
**Zlotnik A.** Chemokines in neoplastic progression. *Semin Cancer Biol*. 2004. Jun;14(3):181-5.

**Zlotnik A.** Involvement of chemokine receptors in organ-specific metastasis. *Contrib Microbiol*. 2006. Jul;13(1):191-9.

## SUPPLEMENTARY CONTENTS

### SUPPLEMENTARY CONTENT – NUMBER 1

#### VEGF-C transcriptomic profile in different organs for *Homo sapiens*



The bar plot shows the transcriptomic expression (transcript per million, TPM) of VEGF-C by whole-tissue RNAseq performed on different organs for *Homo sapiens*. Data for this *in silico* analysis was obtained from HPA (Uhlén 2015) and GTEx (Keen 2015) databases.

Thyroid gland is the organ expressing the highest basal levels of VEGF-C. In case the VEGF-R3 signalling pathway were playing a role on the LNM development, the levels of VEGF-C needed to activate this pathway (this theoretical “threshold” is highlighted as a dotted red line) would be already almost achieved in Thyroid gland, so making this organ more sensitive to LNM, which is consistent with the clinical observation that PTC frequently develops lymphatic metastasis.

## **SUPPLEMENTARY CONTENT – NUMBER 2**

### **Antibodies used for Cell Sorting**

<b>Antibody</b>	<b>Brand</b>	<b>Catalogue</b>	<b>Channel / Fluorophore</b>
Propidium Iodide	BioLegend	421301	Blue 488
CD80	BioLegend	305207	PE 532
CD163	BioLegend	326507	Alexa Fluor® 647

## **SUPPLEMENTARY CONTENT – NUMBER 3**

### **Antibodies used for IHQ**

<b>Antibody</b>	<b>Brand</b>	<b>Catalogue</b>
VEFG-R3	R&D Systems	MAB3491
CD80	BioLegend	305246
CD163	ThermoFisher Scientific	MA5-11458

## SUPPLEMENTARY CONTENT – NUMBER 4

### Primers used for Q-PCR

Target	Forward (5' → 3')	Reverse (5' → 3')
GAPDH	CGTCCCGTAGACAAAATGGT	TTGATGGCAACAATCTCCAC
PPIA	CGCGTCTCCTTCGAGCTGTTG	TGTAAAGTCAACCACCTGGCACAT
VEGF-C	AAGGAGGCTGGCAACATAAC	CCACATCTGTAGACGGACAC
IL-6	ACTCACCTCTTCAGAACGAATTG	CCATCTTTGGAAGGTTTCAGGTTG
IL-12	TCAAACCAGACCCACCGAA	GCTGACCTCCACCTGCTGA
IL-1 $\beta$	AGCTACGAATCTCCGACCAC	CGTTATCCCATGTGTCGAAGAA
IL-10	CAGCCTTGCAGAAAAGAGAGC	CCAGTAAGGCCAGGCAACAT
Snail	AATCGGAAGCCTAACTACAGCGAG	CCTTCCCCTGTCTCATCTGACA
Slug	CCTTCCTGGTCAAGAAGCATTCA	AGGCTCACATATTCCTTGTACAG
Twist	GGCTCAGCTACGCCTTCTC	TCCTTCTCTGGAAACAATGACA

## SUPPLEMENTARY CONTENT – NUMBER 5

### Antibodies used for WB

<b>Antibody</b>	<b>Brand</b>	<b>Catalogue</b>
VEFG-R3	R&D Systems	MAB3491
$\alpha$ -Tubulin	Abcam	ab4074

